Analyzing the Impact of EGFR-induced c-Met Phosphorylation in Non-Small Cell Lung Cancer

by

Austin M. Dulak

B.S. State University of New York at Buffalo 2005

Submitted to the Graduate Faculty of

The School of Medicine in partial fulfillment

of the requirements for the degree of

Doctor of Philosophy.

University of Pittsburgh

2010

UNIVERSITY OF PITTSBURGH

SCHOOL OF MEDICINE

This dissertation was presented

by

Austin M. Dulak

It was defended on

September 16, 2010

and approved by:

Marie C. DeFrances, M.D., Ph.D.
Assistant Professor, Department of Pathology

Jennifer Grandis, M.D.
Professor of Otolaryngology, Department of Pharmacology & Chemical Biology

Jill M. Siegfried, Ph.D.
Dissertation Advisor
Professor and UPMC Chair, Department of Pharmacology & Chemical Biology

Thomas E. Smithgall, Ph.D.
William S. McEllroy Professor and Chair, Department of Microbiology and Genetics

Jack Yalowich, Ph.D.
Associate Professor, Department of Pharmacology & Chemical Biology

Lin Zhang, Ph.D.
Dissertation Committee Chair
Associate Professor, Department of Pharmacology & Chemical Biology

ANALYZING THE IMPACT OF EGFR-INDUCED c-MET PHOSPHORYLATION IN NON-SMALL CELL LUNG CANCER

Austin M. Dulak, Ph.D.

University of Pittsburgh, 2010

Background

Lung cancer is currently the second most prevalent form of cancer in the United States and is the leading cause of cancer-related deaths. Currently, there are no effective therapies for those diagnosed in the later stages of lung cancer. The c-Met receptor is a potential therapeutic target for NSCLC along with its ligand, hepatocyte growth factor (HGF). Signaling interactions between c-Met and the mutant Epidermal Growth Factor Receptor (EGFR) have been studied extensively, but the biological importance of lateral signaling to c-Met in EGFR wild-type tumors is minimally understood.

Principal Findings

Our observations indicate that wild-type EGFR, the receptor most often found in NSCLC tumors, can initiate delayed c-Met activation in NSCLC cell lines. EGFR ligands induce accumulation of activated c-Met which begins at 8 h and continues for 48 h. This effect is accompanied by phosphorylation of critical c-Met tyrosine residues. Gene transcription is required for delayed c-Met activation; however, phosphorylation of c-Met by EGFR occurs without production of HGF or secretion of other factors, supporting an internal mechanism that is independent of c-Met ligand. Lateral signaling is blocked by two selective c-Met tyrosine kinase inhibitors (TKIs), PF2341066 and SU11274, or with

gefitinib, an EGFR TKI, suggesting kinase activities of both receptors are required for this effect. The c-Src pathway is essential for EGFR to c-Met communication. This appears to be up- and downstream of delayed c-Met activation. Pre-treatment with pan-SFK inhibitors, PP2 and dasatinib, abolishes delayed c-Met phosphorylation. A c-Src dominant-negative construct reduces EGF-induced c-Met phosphorylation compared to control, further confirming a c-Src requirement. Additionally, delayed c-Src association with c-Met and prolonged c-Src activation are observed following EGF addition. Inhibition of c-Met with PF2341066 and siRNA decreases the EGF-induced phenotypes of invasion by ~86% and motility by ~81%, suggesting that delayed c-Met activation is utilized by EGFR to potentiate its full biological effects possibly through STAT3. Combined targeting of c-Met and EGFR pathways lead to increased NSCLC xenograft anti-tumor activity.

Conclusions and Significance

Collectively, these data provide an alternative working model of prolonged EGFR signaling, whereby c-Met activation in NSCLC cell lines initiated by wild-type, non-amplified EGFR with wild-type, non-amplified c-Met maximizes EGFR-induced cell motility and invasion. With the identification of this novel pathway, the studies presented here demonstrate that inhibition of both EGFR downstream signaling and EGFR lateral signaling through the EGFR-c-Src-c-Met axis might be effective in treatment of NSCLC. Taken together, these findings will aid in the future development of combination EGFR and c-Met TKI treatments in clinical trials for NSCLC tumors that are wild-type for both EGFR and c-Met.

Table of Contents

LIST OF TABLES

LIST OF FIGURES

PREFACE

A five-year voyage through graduate school is impossible to complete without the aid of numerous individuals for both scientific and emotional support. I owe everyone from the Siegfried Laboratory a thank-you for all of their patience, scientific input, and motivating discussions. An extra special thanks must go to Dr. Laura Stabile and Chris Gubish for all of their help in every facet of my graduate project.

Enormous thank-you to my dissertation advisor, Dr. Jill Siegfried, for years of guidance and for helping me realize my potential as an independent scientist, as well as to my thesis committee for their assistance in the development of this research.

I have saved the biggest plate of thank-you for my friends and family. Bart, you are the only other non-Steelers/Penguins fan in Pittsburgh, and have kept me level headed with our late-night/early morning philosophical discussions about the future of scientific research amongst other things. And for listening to us blabber on and on, Vicki, the landlord. I want to thank the entire Dulak clan for always believing in me, providing me with Buffalo Bills season tickets, and teaching me not to trust everything at face value. Arlee Fafalios, my fiancée, there are no words to describe your never-ending support and encouraging words. Also, for your lessons in writing and speaking brevity: that last sentence has entirely too many words!

1.0 INTRODUCTION

1.1 Lung Cancer Incidence and Risk Factors

Lung cancer has an alarming incidence of 78.5 cases per 100,000 people per year with an expected 222,520 new cases in the United States alone in 2010. The leading cause of cancer-related death in both men and women, lung cancer-related deaths will top 157,000 people this year [1]. In women, the number of lung cancer cases has reached a plateau and remains steady, while the number of male lung cancer cases have been decreasing steadily since the 1990's. Despite this decreasing trend, lung cancer is still a sizeable problem as evidenced by a 5-year survival rate of only 15% [1]. This suggests that although reducing risk factors have decreased the number of cases each year, for those diagnosed with lung cancer, often in its late stages, few effective therapeutic options exist.

The risk factors involved with lung tumorigenesis are well understood with the single greatest risk factor being tobacco product related. The most recent evaluation estimates that 90% of all lung cancer cases are related to primary smoke inhalation from cigarettes, pipes, or cigars and also environmental, second-hand smoke [1]. Moreover, smoking increases the risk of developing lung cancer 10-fold compared to a non-smoker, and this risk increases with the number cigarettes, duration of smoking, and starting age. Additional factors that increase lung cancer risk are other lung diseases such as chronic inflammation, chronic obstructive pulmonary disease (COPD), and pulmonary fibrosis [2]. These diseases, like smoking, are thought to contribute to lung tumorigenesis through

increased inflammation and cell proliferation [3]. Inhalation exposure to environmental agents like radon, arsenic, asbestos, chromates, chloromethyl ethers, nickel, polycyclic aromatic hydrocarbons as well as generalized air pollution are also known causative agents [4, 5]. A purely genetic link has not been fully identified for the development of lung tumors; however, sex differences do appear to play a significant role. Female non-smokers have an elevated risk of developing lung cancer compared to their male counterparts [6]. This observation suggests that steroid hormones and their receptors, such as the estrogen receptor family, play a significant role in increasing susceptibility to lung cancer development and progression, particularly of lung adenocarcinomas [7].

There are two major classifications of lung carcinomas as defined by morphological characteristics, small cell (SCLC) and non-small cell (NSCLC), which NSCLC accounts for nearly 85% of cases [1]. NSCLC is further differentiated by histology into a number of sub-types including squamous cell carcinoma, adenocarcinoma, large cell carcinoma, adenosquamous carcinoma, carcinomas with pleopmorphic sarcomatoid, or sarcomatous elements, carcinoid tumor, carcinomas of salivary-glad type, and unclassified [8]. This methodology of classification provides pathologists and thoracic oncologists with defined characteristics by which to determine more effective treatment regimens.

1.2 Lung Cancer Staging and Treatment

Patients with lung cancer regularly go undiagnosed until late stages of disease (IIIA, IIIB, or IV) due to the lack of a clearly identifiable clinical presentation. Often,

early symptoms of lung cancer are similar to host of other illnesses such as a cough, wheezing, dyspnea, weight loss, and fatigue [9]. Therapeutic options for the treatment of lung cancer, in general, are many, but often ineffective. Currently, treatment options include surgical resection (lobectomy), chemoradiation, and/or chemotherapy with both systemic and targeted agents. The decision to utilize a certain combination of modalities is often defined by lung tumor stage (Table 1) [10-12].

Tumor Stage	Treatment Regimen
I	Surgical resection, radiation
II	Surgical resection, radiation, adjuvant chemotherapy
IIIA	Combination of surgical resection, chemotherapy, and radiation
IIIB	Chemotherapy and radiation
IV	Doublet of chemotherapy or clinical trials with novel agents

Table 1. Lung tumor staging and treatment options.

Tumor stage is defined by a number of characteristics including tumor size, regional lymph node involvement, and metastases, both regional and distant as measured by computed tomography (CT) screening, bronchoscopy, and occasionally magnetic resonance imaging (MRI) [5]. Methodology of surgical resection and chemoradiation are focused on removing or destroying as much of the tumor as possible, while minimizing damage to surrounding tissues. Chemotherapy regimens rely on the ability to destroy the rapidly proliferating tumor cells preferentially over normal cells with a slower rate of turnover.

Initially, lung cancer patients were treated with first-generation therapies alone such as platinum-based agents (cisplatin and carboplatin); however, with the emergence of known resistance mechanisms, these older chemotherapies are now often combined

with later-generation cytotoxic drugs such as taxanes (paclitaxel and docetaxel), vinorelbine, gemcitabine, irinotecan, and pemetrexed to produce slightly better response rate and improved survival. The modest improvement for these combinations was approximately a 15% increase in response rate and about a 1-2 month increase in survival [10-12]. Through these results and many others like it, it became evident that novel modes of therapeutic targeting were necessary to further improve patient response and survival time while decreasing toxic side effects. The hypothesis of a cancer "magic bullet" or targeted drug that is cancer-specific remained omnipresent for a long while, but only as recent as the 1990's has this theory come to fruition.

Initial findings of cancer-targeted agents were identified in the late 1990's when Brian Druker at the Ohio State University measured an exciting response to imatinib the ATP-competitive, tyrosine kinase inhibitor (TKI) in chronic myeloid leukemia (CML). Analysis determined that imatinib inhibited uncontrolled proliferation by blocking the driving force for proliferation and progression in many CML soft tumors, the protein tyrosine kinase fusion protein, BCR-ABL. This observation led to the purchase of imatinib by Novartis [13]. Since this seminal finding, there have been strong efforts to identify cancer-specific genes involved in tumorigenesis and progression. In the case of lung cancer, and NSCLC specifically, many novel targets have been identified and more are being measured each year. The most hopeful and promising target to date has been the Epidermal Growth Factor Receptor (EGFR), which is overexpressed in many cancers including 80-85% of NSCLC tumors [14]. Overexpression of EGFR is correlated with poor prognosis and decreased survival and believed to be one of the major driving forces in NSCLC progression through hyper-activation [15, 16].

1.3 Epidermal Growth Factor Receptor

1.3.1 EGFR Activation and Function

EGFR (ErbB1) is a member of the structurally-related erbB family of receptor tyrosine kinases (RTK) that also includes HER2/Neu, HER3 and HER 4, and was named for the oncogene encoded by the avian erythroblastosis virus [17]. Many, if not all, normal epithelial cells express the mature 170 kDa ErbB1 gene product, but in NSCLC tumors the receptor is often overexpressed [14]. Activation of EGFR occurs not only through interaction with EGFR ligands epidermal growth factor (EGF), transforming growth factor-alpha (TGF-α), amphiregulin (AR), beta-cellulin, HB-EGF, and epiregulin, but also through interactions with other RTKs and G-protein coupled receptors [18, 19]. These interactions with EGFR ligands, probably as dimers, brings two EGFR monomers in close proximity to form an EGFR homodimer, or EGFR can heterodimerize with other monomers from the erbB family such as HER2 or HER 3 [20]. Trans-autophosphorylation within the intracellular tyrosine kinase domain activates the tyrosine kinase activity of EGFR and allows for subsequent downstream tyrosine phosphorylation of multiple tyrosine residues in the carboxy-terminal tail. These phospho-tyrosine residues then serve as docking sites for interaction with Src Homology-2 (SH2) and phospho-tyrosine binding (PTB) domain-containing proteins such as growth factor receptor-bound protein 2 (Grb2), Shc, and phospholipase C-γ (PLCγ), and c-Src [21-26]. EGFR interaction with these adaptor molecules allows for amplification and downstream

transmittance of the initial activating signal to modulate central effector molecules that regulate cell proliferation, invasion, motility, survival, and angiogenesis such as the RAS/mitogen-activated protein kinase (MAPK) cascades, phosphatidylinositol 3-kinase (PI3K)/Akt, and signal transducer and activator of transcription (STAT) family of proteins (Fig. 1) [27]. Because of EGFR hyper-activation in NSCLC tumors and upstream involvement in many signal transduction pathways that contribute to tumor development and progression, many targeted drugs such as TKIs and monoclonal antibodies were designed to inhibit EGFR action.

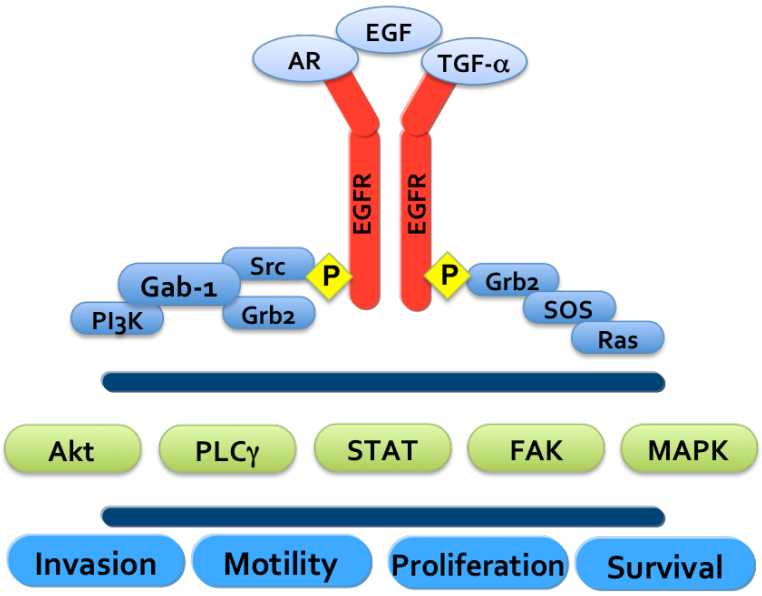

Figure 1. EGFR signal transduction pathway.

1.3.2 EGFR Targeted Therapeutics

The chimeric monoclonal antibody, cetuximab (C-225, brand name: Erbitux), was the first neutralizing antibody developed to impede EGFR action in colorectal cancer

[28]. Binding to the extracellular domain of EGFR, cetuximab inhibits the ligand binding interaction between EGFR and it natural ligands preventing downstream signal transduction. Because this biological entity demonstrated high efficacy against colorectal tumors, it was moved into early phase clinical trials as a first-line treatment of NSCLC. Initial phase II and III trials comparing cetuximab combined with or without cisplatin and vinorelbine demonstrated increased response rate and a statistically significant improved overall survival [29]. However, additional evidence is required to gain full approval for the use of cetuximab in the treatment of NSCLC, and these trials are currently ongoing.

EGFR TKIs, to date, are the strongest and most encouraging endeavors into blocking EGFR signaling in NSCLC tumors. In 2003, the FDA approved gefitinib (ZD1839, brand name: Iressa) for the treatment of advanced NSCLC after other treatment options failed [30, 31]. Developed by AstraZeneca, gefitinib is an orally available member of the analino-quinazoline family of molecules that reversibly competes with ATP at the ATP binding pocket of EGFR [32, 33]. By preventing ATP from binding to EGFR, EGFR tyrosine kinase activity cannot be initiated and tumorigenic signaling is unable to proceed. The specificity and potency of gefitinib towards EGFR activation was the most remarkable hallmark of this drug. EGFR activation as assessed through *in vitro* kinase assays was inhibited with an IC_{50} = 0.033μM. The next closest assessed targets were HER2, KDR, and FLT-1 that had IC_{50} concentrations 100-fold higher than what was observed with EGFR [34]. Efforts in cell and animal models provided promising results; however, clinical outcome did not match these preclinical expectations.

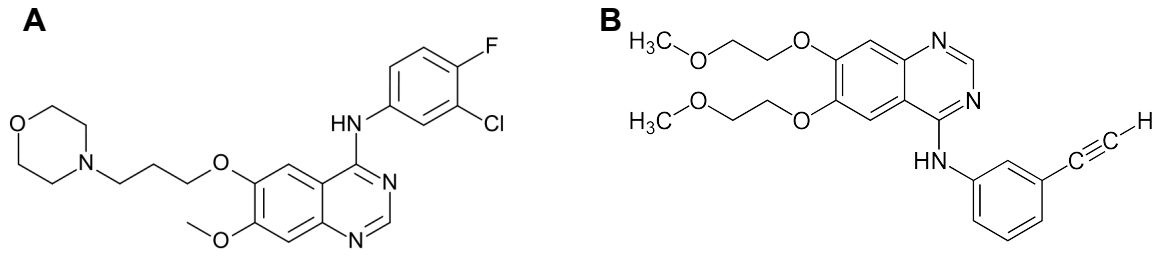

Figure 2. Chemical structures of gefitinib (A) and erlotinib (B).

Initially, gefitinib was utilized as a single therapy in NSCLC patients that were resistant to platinum-based chemotherapies and docetaxel. The results from these initial studies found that tumor response were about 18% with symptom improvement observed in 40% of patients [30, 31]. Because of these findings, gefitinib was approved for use as a first-line therapy combined with cytotoxic chemotherapies in NSCLC patients. Unfortunately, this combination regimen failed to improve overall survival, time to progression, or response rate compared to chemotherapy alone [35, 36]. It was later determined that patients with tumors with EGFR mutations benefitted from gefitinib therapy due to increased ATP binding pocket affinity, while tumors with EGFR wild-type receptor lacked sensitivity. This will be elaborated on further later in the introduction. Currently in the United States, gefitinib is used sparingly and is only available to patients that have benefitted from gefitinib therapy in the past.

Not long after these clinical observations, another EGFR TKI developed by Genentech and OSI Pharmaceuticals, erlotinib (OSI-774, brand name: Tarceva), was approved by the FDA for treatment of NSCLC patients that have failed at least one prior

chemotherapy regimen [37]. Like gefitinib, erlotinib is also an orally-available, analino-quinazoline-derived ATP competitive EGFR inhibitor with an IC_{50} = 0.002 μM [38]. In the clinical setting, erlotinib exhibited early promise by showing significantly longer progression-free survival and overall survival compared with placebo in patients with advanced NSCLC who previously received prior chemotherapy [39]. But as with gefitinib, many resistance and escape pathways decreased the efficacy in large populations. Still, erlotinib is approved in the United States for treatment of NSCLC due to some evidence suggesting that EGFR wild-type tumors benefit from erlotinib monotherapy and is utilized in patients with EGFR activating mutations.

1.3.3 EGFR Tyrosine Kinase Inhibitor Resistance

Retrospective analysis demonstrated various ways utilized by tumor cells to escape inhibition by EGFR TKIs including both intrinsic and acquired mechanisms. This is particularly important in the treatment of NSCLC tumors expressing wild-type EGFR, which comprises the majority of NSCLC patients, and these tumors show intrinsic resistance [40]. One of the most prominent modes by which cancer cells circumvent RTK targeted therapy is to divert critical signal transduction pathways to other RTKs. This is possible due to the high level of RTK redundancy that leads to activation of downstream pathways involved in tumor progression. Among these, RTKs such as c-Met and insulin-like growth factor-1 receptor (IGF-1R) can activate overlapping signaling cascades to continually signal to effector molecules such as MAPK and Akt in the event of EGFR blockade [41, 42]. Also, constitutive activation of molecules downstream of EGFR can

cause resistance to EGFR TKIs, particularly those of the KRAS gene with mutations in codons 12 and 13. These activating mutations occur in 15-20% of lung cancer patients and are associated with poor prognosis independent of therapy [43, 44]. Tumors harboring KRAS activating mutations are unlikely to be sensitive to EGFR therapy as the tumor driving force for growth through MAPK is downstream of receptor activation [40]. Secondary mutations in EGFR itself also confer resistance to inhibition by either gefitinib or erlotinib in patients with primary EGFR mutations. The most common EGFR TKI resistant mutation is the T790M gatekeeper mutation that occurs in 50% of patients [45-48]. This mutation within the ATP binding pocket of EGFR is thought to sterically block the binding to EGFR TKIs, but still allow binding of ATP into the ATP binding pocket, resulting in EGFR phosphorylation and activation.

More recently, MET amplification was observed as an important escape mechanism in NSCLC that contain EGFR mutations. MET gene amplification is a mode of acquired EGFR TKI resistance that expands upon the previously mentioned intrinsic mechanisms of overlapping pathways. EGFR and c-Met both initiate anti-apoptotic, pro-survival signaling through the HER3 activation of the PI3K/Akt pathway in lung tumor cells. In the presence of EGFR inhibition, MET amplification is selected for in tumor cells resulting in a greater c-Met receptor density such that signaling to HER3 can proceed in the absence of EGFR input [42]. This mode of resistance combined with the EGFR T790M mutation accounts for 60-70% of all acquired EGFR TKI resistance and the two are not mutually exclusive [49]. For this and other reasons, c-Met along with its ligand, Hepatocyte Growth Factor/Scatter Factor (HGF), is being studied as a possible target for NSCLC therapeutic development.

1.4 Hepatocyte Growth Factor and c-Met

1.4.1 HGF and c-Met Structure

HGF is produced and secreted by mesenchymal cells such as fibroblasts and was initially identified as a platelet-derived mitogen for hepatocytes and a factor capable of inducing epithelial cell scattering, similar to that observed during epithelial-to-mesenchymal transition [50, 51]. The HGF gene located on chromosome 7q21.1 encodes a precursor HGF molecule that is cleaved to a mature form by a protease [52]. The activated HGF protein binds with the RTK c-Met to exert its function.

C-Met is a plasma membrane bound RTK encoded by the MET proto-oncogene at the 7q21-q31 locus that shares similar structural homology to RTKs Ron and Sea. The receptor is expressed in all normal epithelial cells as well as some endothelial cells [53].

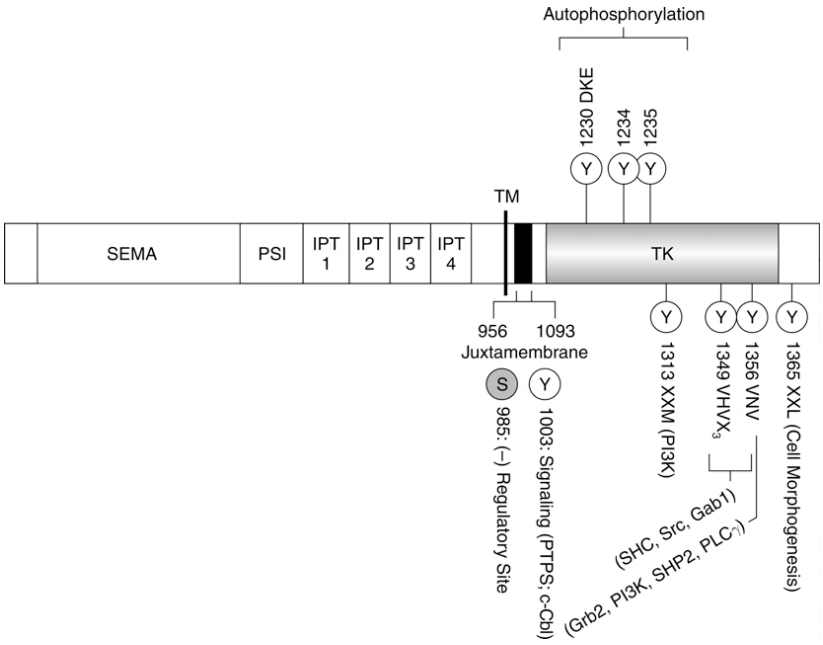

Figure 3. Structure of c-Met and important phosphorylation sites (Ma, PC, *et al.* 2003).

Produced as a 150 kDa polypeptide, c-Met undergoes a number of post-translational glycosylation steps to become the fully mature 170 kDa pro from of c-Met. The pro-c-Met molecule is cleaved into two subunits, a 45 kDa extracellular α-chain and a 145 kDa β-chain that has both extracellular and intracellular domains, that are linked through a disulfide bridge to form the mature c-Met receptor. The binding pocket for HGF on each c-Met monomer consists of the α-chain and the extracellular region of the β-chain, while the intracellular portion of c-Met contains the juxtamembrane and tyrosine kinase domains (Fig. 3) [54].

1.4.2 C-Met Activation and Signal Transduction

The interaction between HGF and c-Met occurs in a paracrine, endocrine, or autocrine manner [50, 51, 55, 56]. In a canonical pathway, HGF ligand binding, probably as a dimeric molecule, brings two c-Met heterodimeric units in close proximity to induce trans-autophosphorylation in the tyrosine kinase domain of the intracellular β-chain of c-Met, similar to EGFR. Specifically, the tyrosine residues Y1230, Y1234, and Y1235 are critical for c-Met tyrosine kinase activity [57, 58]. This activation leads to subsequent phosphorylation on tyrosine residues Y1349 and Y1356 in the carboxy-tail which, comprise the multi-substrate docking site (MSDS), is integral in c-Met function, and allows recruitment of effector molecules responsible for downstream signaling such as GRB2-associated-binding protein 1 (Gab1), PI3K, Grb2 and c-Src [54, 57-59]. Additionally, phosphorylation of Y1365 regulates cell morphogenesis, and Y1003 is important for internalization and proteosomal degradation of c-Met through interaction with the E3 ubiquitin ligase, c-Cbl (Fig. 3) [60]. These protein-protein interactions with c-Met are carried out through SH2, PTB, and Met binding domains (MBD) and are necessary for c-Met pathway activation. The role of the effector molecules is to diversify the initial phospho-c-Met signal by creating additional docking sites for effector molecules.

Signal transduction cascades activated by RTKs such as c-Met rely on phosphorylation, whether it be on tyrosine, serine, or threonine residues, downstream to activate transcription factors. In turn, these transcription factors upregulate genes critical for phenotypic modulation. In the case of c-Met, the phenotypic modulation takes the

form of a program requiring precise coordination of growth, invasion, motility, anti-apoptosis, and angiogenesis, termed invasive growth [61]. Each individual phenotype typically relies heavily on compound pathways that are central to one pathway or molecule. For proliferation and cell growth, the critical pathway activated by RTKs is the Ras/MAPK cascade. This pathway ultimately is initiated in a rapid and transient manner and signals downstream for the activation of the Erk1/2 and upregulation of cyclin D1 and c-Myc [62]. The integrin family, c-Src/focal adhesion kinase (FAK), upregulation of matrix metalloproteinases (MMPs), and downregulation of E-cadherin are key steps in signaling that leads to increased cell motility and invasiveness [63]. As briefly discussed earlier, the PI3K/Akt pathway is critical in cell survival especially to prevent anoikis [64, 65]. HGF upregulates angiogenesis through mechanisms central to cyclooxygenase-2 (COX-2) upregulation, vascular endothelial growth factor (VEGF), and interleukin-8 (IL-8) production [66]. The STAT family of transcription factors including STAT3 are key components of multiple cellular processes such as proliferation, survival, and invasion [67, 68]. As a whole, these HGF/c-Met phenotypes are utilized in normal physiological processes, but are hijacked by tumor cells for uncontrolled invasive growth (Fig. 4).

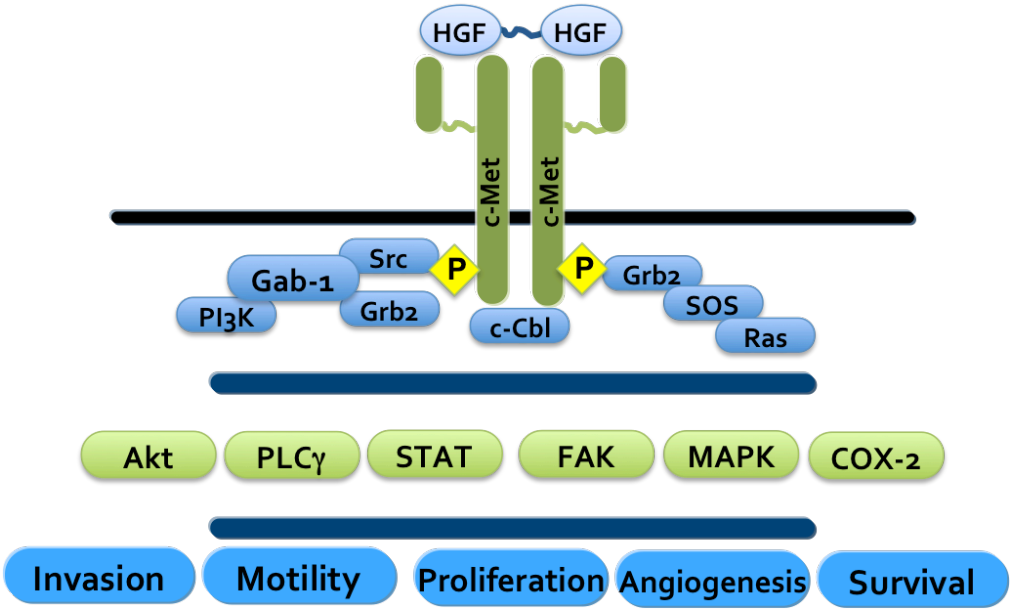

Figure 4. HGF/c-Met signal transduction pathway.

1.4.3 C-Met Activation through Cross-talk Mechanisms

Not only is c-Met activated in response to HGF ligand interaction, but also through mechanisms of cross-talk or lateral signaling from other cell surface protein families. Among these are G-protein coupled receptors (GPCR), integrins, class B plexins, CD44, Ron, HER3, and most notably, EGFR. The manner in which these molecules interact with and activate c-Met vary greatly, but two general modes are utilized: indirect and direct. For example, integrin clustering can induce HGF-independent phosphorylation of c-Met, likely through an indirect signaling pathway, in mouse melanoma cells [69-72]. Cross-talk between the transmembrane protein, CD44, and c-Met is dependent on HGF binding. The CD44 variant 3 isoform is a heparin sulfate binding protein that is shown to interact on the cell surface with HGF. This interaction allows the presentation of HGF to c-Met [73, 74]. GPCR agonists lysophosphatidic acid

(LPA), bradykinin, thrombin, and carbachol can induce c-Met phosphorylation through c-Met ectodomain shedding [75]. In theory, this process of extracellular removal would allow the remaining intracellular c-Met fragments to dimerize resulting in c-Met trans-autophosphorylation. Glial cell line-derived neurotrophic factor (GDNF) can also activate c-Met upon interaction with its cognate receptor, RET. The mechanism responsible for this is central to c-Src, but c-Src is not thought to be directly phosphorylating c-Met [76]. As a whole, these molecules provide a representative picture of the various mechanisms involved in c-Met activation. It does appear that these interactions are necessary for cell invasion, placing c-Met as the central modulator of this invasive growth phenotype [77].

C-Met and EGFR cross-talk has been well-documented and continues to be actively studied due to roles of both RTKs in oncogenic transformation and therapeutic development. C-Met is frequently co-expressed with EGFR family members in human tumors, and it has been demonstrated that these RTKs can signal to one another [75, 78-81]. Presnell *et al*. first showed that c-Met could be trans-activated by EGFR in rat liver epithelial cells constitutively expressing TGF-α [81]. Similar studies have since observed this signaling in NSCLC tumor models where EGFR contains activating mutations such as L858R or E746-A750del [82]. Additionally, lateral signaling to c-Met from EGFR has been identified in EGFR wild-type models, and much of this data suggests that cross-communication from EGFR to c-Met is dependent on EGFR or c-Met expression levels [83, 84]. To further validate this mechanism, Xu *et al*. recently demonstrated that induction of c-Met phosphorylation required upregulation of c-Met through EGFR-activated hypoxia-induced factor 1-alpha (HIF-1α) in both EGFR wild-type and mutant

cell lines [85].

Depending on the cell model system employed, a wide-spanning number of mechanisms can initiate this cross-talk between EGFR and c-Met. In NSCLC and epidermal carcinoma cell lines, c-Met and EGFR are in a signaling complex as identified through co-immunoprecipitation studies [78, 82]. It is unclear whether this interaction forms a c-Met/EGFR heterodimer or whether this is an indirect complex of a c-Met homodimer with an EGFR homodimer. The structural requirements for c-Met dimerization suggest that this observed association is indirect due to lack of SEMA domain homology in EGFR [86]. Also, EGFR can activate cell surface proteases through the MAPK pathway that induce c-Met ectodomain shedding similar to GPCR activation of c-Met [75]. C-Src appears to play an important, yet not fully defined, role in cross-talk as well. Mueller *et al*. demonstrated that in breast cancer cells c-Met activates the non-receptor tyrosine kinase, c-Src, which in turn can directly phosphorylate EGFR allowing for signal attenuation [87]. In our laboratory, we previously demonstrated that exogenous prostaglandin E2 (PGE_2), stimulated invasion in our NSCLC model system through an intricate signaling axis requiring EGFR ligand production, c-Met, and the Src family kinases (SFK) [88]. Thus, this provides circumstantial evidence that EGFR activation of c-Met requires c-Src in some capacity in NSCLC. Despite these many findings, few studies have dissected the exact role of c-Src in EGFR/c-Met cross-talk, and the biological outcomes of such an interaction.

1.4.4 C-Met Function in Normal Tissues

In normal tissues, the HGF/c-Met pathway is critical for embryonic development and tissue regeneration, where both processes utilized regulated invasive growth. During mouse embryogenesis, HGF and c-Met are co-expressed in endodermal and mesodermal structures along the rostro-caudal axis [89]. HGF and c-Met are absolutely required for placenta and liver development and for directional migration of myoblasts from somites to the limbs [90]. The essential requirement for these two molecules in development is highlighted by separate studies demonstrating that HGF and c-Met knockout mice share similar phenotypes and are both embryonically lethal [91, 92].

Invasive growth, in adult tissues is generally quiescent; however, it can be reactivated by sensing organ damage when remaining cells must migrate to reconstitute the integrity of the injured tissues. Following injury to liver, heart, or the kidney, HGF levels increase in plasma due to secretion from both local and distant sites [93-96]. Upon tissue regeneration, the invasive growth program is canceled and HGF and c-Met levels decrease to basal level conditions. This cancelation process after these normal processes highlights the explicit difference in physiological invasive growth from uncontrolled invasive growth in cancer cells.

1.4.5 HGF/c-Met Pathway in Cancer

HGF/c-Met dysregulated signaling has been implicated in many cancers including NSCLC [63]. The first evidence that c-Met activation could lead to oncogenic

transformation was with the identification of the translocated promoter region (TPR)-MET fusion protein that was a product of a chromosomal rearrangement in an osteosarcoma cell line treated with chemical carcinogen that caused c-Met to be constitutively active [97]. Since then other mechanisms of dysregulation including, HGF and/or c-Met amplification, c-Met activating mutations, and HGF autocrine signaling loops were observed [98]. In the case of NSCLC, overexpression of HGF and/or c-Met is the leading driver of aberrant activity potentially through increased receptor oligomerization and ligand-independent activation [63]. Additionally, it was observed that certain juxtamembrane mutations in the c-Met receptor confer prolonged activation and signaling due to loss of the Y1003 phospho-tyrosine residue required for regulating internalization [99]. Aberrant activation of the HGF/c-Met pathway is uncontrolled; thus, this pathway is an ideal candidate for therapeutic intervention. Disruption of the HGF/c-Met pathway by c-Met-directed siRNAs, therapeutics, and HGF antibodies decreases tumorigenic potential [51, 100-102]. Based on these studies and findings that the HGF/c-Met pathway contributes to EGFR TKI resistance, there have been strong efforts to develop therapies to block this pathway in many cancers including NSCLC [98].

1.4.6 HGF/c-Met Targeted Therapeutics

Development of therapeutic strategies targeting the HGF/c-Met pathway is currently under rapid development by academic institutes and industry, alike. The most common targeted molecules designed to antagonize this pathway are HGF- or c-Met-specific monoclonal antibodies and ATP competitive inhibitors against c-Met [98, 102].

Rationally designed neutralizing monoclonal antibodies directed against HGF and c-Met are focused on disrupting the HGF interaction with c-Met at the HGF binding pocket. Through disruption of this binding, c-Met activation through the canonical ligand pathway cannot proceed and c-Met regulated invasive growth is abolished [102]. These directed therapeutics are currently in the early stages of clinical trials with more being disclosed yearly.

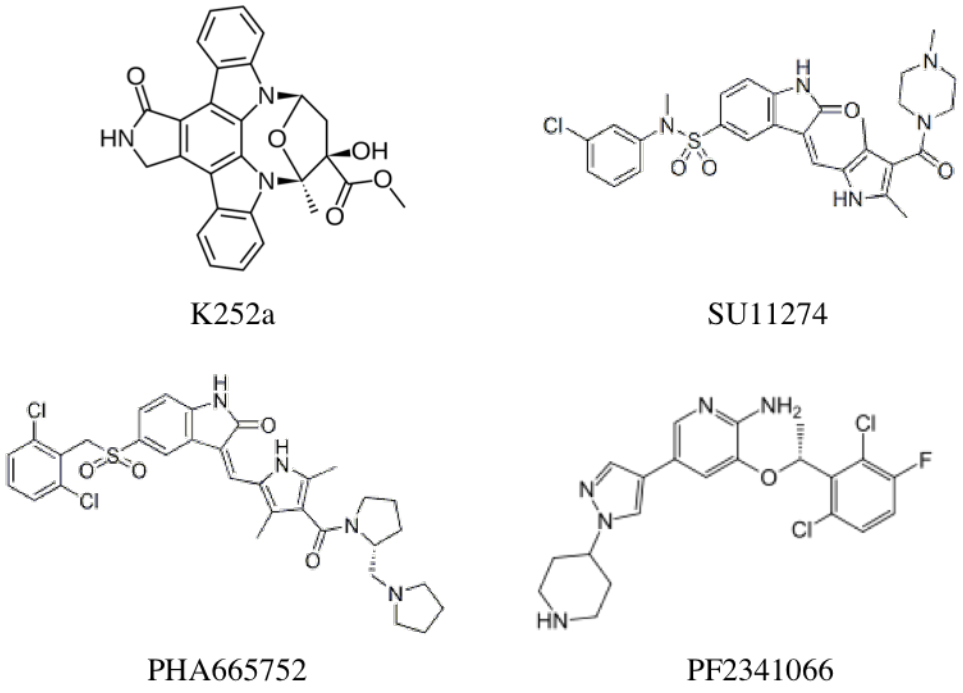

Figure 5. Chemical structures of c-Met targeted agents.

To date, a majority of HGF/c-Met pathway specific inhibitors are c-Met directed TKIs that function similar to gefitinib and erlotinib targeting of EGFR. The initial molecule identified to impede c-Met activation was the staurosporine analog and Trk family inhibitor, K252a (Fig. 5). K252a inhibited HGF-induced cell scattering was relatively low at 30 nM, but also had extensive off-target effects on other tyrosine kinases such as

platelet-derived growth factor receptor (PDGFR) [103]. Despite, the lack of specificity of K252a, these findings provided a strong foundation for the development of other small molecule c-Met inhibitors such as SU11274, PHA665752, and PF2341066 (Fig. 5).

SU11274 and PHA665752 were Pfizer's first reported c-Met ATP competitive inhibitors. These molecules share a similar indolin-2-one core structure with differing R-group substitutions and are potent inhibitors of c-Met in enzymatic assays: SU11274 IC_{50}=0.01 μM, PHA665752 IC_{50}=0.009 μM. The specific interaction of these inhibitors with c-Met is not perfectly understood, but it is known that SU11274 activity is lost in cells with a c-Met Y1248H mutations suggesting that interaction with the activation loop is key for compound activity [104]. In biochemical studies, these preclinical molecules can inhibit c-Met autophosphorylation in cell model systems. SU11274 blocked c-Met phosphorylation at a 5 μM concentration in A549 cells and, the later generation, PHA665752 inhibited phosphorylation at a 1 μM concentration [104, 105]. Both molecules also demonstrated *in vivo* efficacy by reducing xenograft tumor growth; however, both molecules failed to move into clinical trials due to lack of bioavailability and poor pharmaceutical properties.

Pfizer moved forward with development of PF2341066 (crizotinib), a more selective and potent c-Met inhibitor (IC_{50}=0.004 μM). This member of the pyridine family also had significant specificity (IC_{50}=0.024 μM) on the anaplastic lymphoma kinase (ALK). Cell-based assays demonstrated that concentrations between 5 nM and 20 nM inhibited c-Met-dependent phenotypes of proliferation, migration, and invasion, as well as reduced lung xenograft tumor growth at a dosages between 6.25 mg/kg/day and 50 mg/kg/day in multiple cancer models [106, 107]. Because of these exciting findings,

this inhibitor moved rapidly into clinical trials for NSCLC. In a phase I trial, PF2341066 showed high clinical efficacy against tumors with activating ALK gene fusions or MET alterations [108]. Ongoing phase II and III clinical trials are currently assessing the efficacy of this molecule with the anticipation that it will be selectively utilized in lung tumors that have MET amplification or express the hyper-active Echinoderm microtubule-associated protein-like 4 (EML4)-ALK fusion gene. Both of these factors render the tumor cells highly sensitive to this agent. Concurrently, there remain strong efforts to identify additional molecules to target the HGF/c-Met pathway in lung cancer especially to combine with EGFR TKIs to circumvent resistance [42, 109, 110].

1.5 Personalized Medicine in Lung Cancer

It was initially thought that EGFR overexpression as detected by immunohistochemistry might correlated with EGFR TKI sensitivity; however, recent studies suggest that EGFR mutations in NSCLC not only render tumors resistant, but also can increase sensitivity to EGFR TKIs. As discussed previously, the EGFR T790M gatekeeper mutation decreases sensitivity of NSCLC cells to the EGFR small molecule inhibitors erlotinib and gefitinib. Conversely, EGFR activating mutations such as the in-frame deletion in exon 19 (E746-A750del) and the substitution of arginine for leucine at position 858 (L858R) causes increased sensitivity to EGFR TKIs [48]. Approximately 70% of tumors expressing EGFR activating mutations are sensitive to EGFR TKI treatment compared to a 10% response in EGFR wild-type tumors [111]. These seminal findings along with the improvement in sequencing technologies and proteomic profiling

have provided intriguing opportunities to tailor specific treatments for patients based on molecular characteristics of individual tumors.

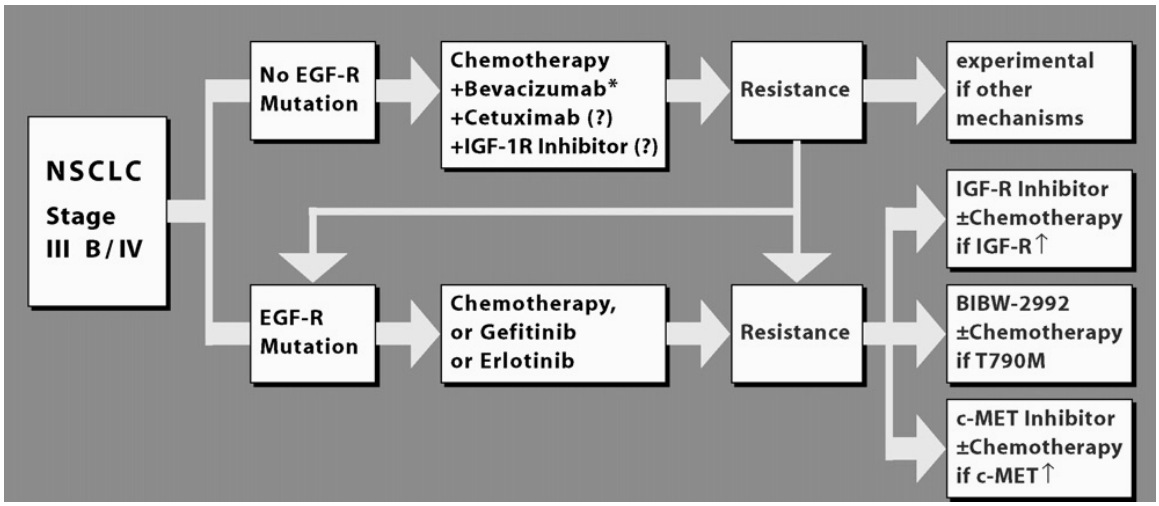

Figure 6. Example of NSCLC treatment algorithm. (Dempke, WCM, *et al.* 2010)

Personalized medicine in the context of late stage (IIIA, IIIB, and IV) NSCLC is making progress through response analysis of patients treated with targeted agents. A present focus in NSCLC is to characterize the specific driving forces responsible for individual tumor growth. Currently, it is believed that that less than 10% of NSCLC tumors are driven by EGFR mutations, about 10% through KRAS mutations, 3.5% through the EML4-ALK fusion protein, 1.5% BRAF, 3% other (PI3K, HER2), and others yet to be identified [43, 112-115]. These mutations are particularly observed in lung adenocarcinomas. Once this profiling of tumors is more complete, it will provide pathologists and oncologists with a more comprehensive treatment algorithm to base therapeutic strategy decisions compared to the current usage of histological markers alone (Fig. 6). For example, a tumor with a KRAS mutation with no EGFR mutation would likely be resistant to any RTK targeting with c-Met and EGFR agents. Therefore,

an inhibitor of effector molecules downstream of KRAS such as MEK, using the inhibitor AZD6244, might be a more beneficial target [116] An additional example applies to NSCLC tumors expressing wild-type EGFR with increased c-Met activity through elevated HGF levels. According to this profile, the first-line course of action might be to combine EGFR and c-Met TKIs to inhibit tumorigenic signaling from both receptors as well as the known resistance development.

As profiling technologies become more affordable and ubiquitous, a flow-chart such as the one depicted here could further guide effective treatment regimens. With the vast number of targeted agents available for NSCLC treatment, and many more in development, the future focus is to identify sensitive populations of individuals that might respond to selective treatment.

1.6 PURPOSE

It is our overall hypothesis that stimulation of c-Met through both HGF and lateral signaling from the EGFR pathway is important in lung cancer:

1) Determine the mechanism by which EGFR activation of c-Met occurs.
2) Understand the biological consequences of EGFR to c-Met communication.
3) Investigate the advantage of combination treatment targeting c-Met and EGFR in a bioluminescent orthotopic murine model of NSCLC.

Upon successful completion of the proposed aims, we will gain a better understanding of critical intermediates in this additional pathway that leads to c-Met activation, and this

knowledge will be utilized as rationale for the clinical development of novel c-Met/EGFR combination strategies in EGFR and c-Met wild-type NSCLC.

1.7 MATERIALS AND METHODS

1.7.1 Chemical Reagents

Actinomycin D, SU11274, and PP2 were purchased from Calbiochem (San Diego, CA). Dasatinib (BMS-354825) was purchased from Chemietek (Indianapolis, IN). The c-Met and non-targeting siRNA ON-TARGET*plus* SMARTpools were purchased from Dharmacon (Lafayette, CO). EGF, TGF-α, HGF, HGF neutralizing antibody, and non-immune IgG control were purchased from R&D Systems (Minneapolis, MN).

1.7.2 Cell Lines and Culture Conditions

NSCLC cell lines A549 and H1435 were obtained from American Type Culture Collection (Manassas, VA) and the 201T cell line was established in our laboratory from primary tissue specimens [117]. All cells were maintained at 37°C in 5% CO_2. All cells were grown in Basal Medium Eagle (BME) or RPMI 1640 supplemented with 10% fetal bovine serum and 2 mM L-Glutamine. All cells were grown to 60-80% confluence in full

serum media and serum-deprived 48 h prior to growth factor stimulation unless otherwise noted.

1.7.3 Protein Analysis

Immunoprecipitation

Equal amounts of protein was subjected to immunoprecipitation with indicated antibodies overnight at 4°C while rotating then incubated with Protein A-Agarose Beads (Thermo Fisher Scientific, Rockford, IL) for 2 h at 4°C. Samples were washed 3X with NP-40 lysis buffer (50 mM Tris-HCl, 150 mM NaCl, 1% NP-40, pH 8.0) containing a Complete Mini Protease Inhibitor Cocktail Tablet (Roche, Indianapolis, IN) and phosphatase inhibitors (25 mM NaF and 1.5 mM NaV) and resuspended in 2X Tris-Glycine SDS Sample Buffer (0.5 mM Tris-HCl, 20% Glycerol, 10% SDS, 0.1% Bromophenol Blue).

Western Blotting

Cells were washed with twice with 1X phosphate-buffered saline (PBS) and lysed with NP-40 lysis buffer and briefly sonicated. The insoluble fraction was cleared by centrifugation at 10000 x g for 15 min at 4°C. Protein concentrations were measured by Bradford Assay (Pierce). Equal amounts of protein were separated on Tris-Glycine SDS page gels under reducing conditions. Protein was transferred to nitrocellulose membrane followed by blocking with 5% milk, 1x Tris-Buffered Saline (TBS) with Tween 20. Primary antibodies were incubated in 1% milk, 1x TBS-Tween 20 at 4°C overnight. Secondary antibodies were horseradish peroxidase–conjugated IgG at a 1:2,000 dilution.

ECL Plus chemiluminescent (GE Healthcare, Piscataway, NJ) was used for detection followed by autoradiography. For re-probing, blots were stripped using IgG Elution Buffer (Thermo Fisher Scientific). Blots were quantified by densitometry and ImageJ analysis (National Institutes of Health, Bethesda, MD).

Primary Antibodies

Primary Antibody	**Species; Dilution**	**Manufacturer**
Phospho-c-Met (Y1349)	Rabbit; 1:1000	Invitrogen (Carlsbad, CA)
Phospho-c-Met (Y1365)	Rabbit; 1:1000	Invitrogen
Phospho-c-Met (Y1003)	Rabbit; 1:1000	Invitrogen
Phospho-c-Src (Y418)	Rabbit; 1:1000	Invitrogen
Total c-Src	Mouse; 1:1000	Invitrogen
Total c-Met (C-28)	Rabbit; 1:1000	Santa Cruz Biotechnology (Santa Cruz, CA)
Total c-Src (N-16)	Rabbit; 1:1000	Santa Cruz Biotechnology
Phospho-tyrosine (pY99)	Mouse; 1:750	Santa Cruz Biotechnology
Total c-Met (C-12)	Rabbit; 1:150	Santa Cruz Biotechnology
Total Lyn	Rabbit; 1:1000	Santa Cruz Biotechnology
Total c-Met (25H2)	Mouse; 1:1000	Cell Signaling (Beverly, MA)
Phospho-EGFR (Y1068)	Mouse; 1:1000	Cell Signaling
Total EGFR	Rabbit; 1:1000	Cell Signaling
Phospho-c-Met (Y1234/35)	Rabbit; 1:1000	Cell Signaling
P44/42 MAP Kinase	Rabbit; 1:1000	Cell Signaling
Phospho- p44/42 MAP Kinase (E10)	Mouse; 1:1000	Cell Signaling
Phospho-Akt (S473)	Rabbit; 1:1000	Cell Signaling
Total Akt	Rabbit; 1:1000	Cell Signaling

Phospho-Stat3 (Y705)	Rabbit; 1:1000	Cell Signaling
Total Stat3	Rabbit; 1:1000	Cell Signaling
Total MMP2	Rabbit; 1:500	Santa Cruz Biotechnology
Total MMP9	Rabbit; 1:500	Santa Cruz Biotechnology
Total EGFR	Mouse; 1:1000	BD Transduction Laboratories (San Jose, CA)
E-Cadherin	Mouse; 1:500	BD Transduction Laboratories
Total EGFR	Mouse; 1:7500	Sigma-Aldrich
β-Actin	Mouse; 1:50000	Sigma-Aldrich
Ki-67	Rabbit, 1:200	Abcam (Cambridge, MA)
COX-2	Mouse; 1:1000	Cayman Chemicals (Ann Arbor, MI)

1.7.4 Analysis of HGF Expression

Human HGF ELISA

Cell culture media was harvested and analyzed in triplicate by Quantikine Human HGF enzyme-linked immunosorbent assay (ELISA; R&D Systems) according to the manufacturer's instructions. Conditioned media from fibroblasts was used as a positive control for HGF levels.

Quantitative Real Time-PCR

Total RNA was extracted using the RNAeasy kit (Qiagen, Valencia, CA) according to manufacturer's directions. CDNA was synthesized by reverse transcription in the presence of 3.5 mM $MgCl_2$ in a thermocycler. TaqMan assay was performed in a 7700 Sequence Detector (Applied Biosystems, Foster City, CA) with an initial denaturation of

12 min at 95 °C followed by 40 cycles of 15 s of denaturation at 95 °C and 60 s of annealing and extension at 60 °C. The primers and probes used for detection are: validated HGF and c-Met Taqman primer/probe mix was purchased from Applied Biosystems, β-GUS: forward primer (5'-CTCATTTGGAATTTGCCGATT-3'); β-GUS reverse primer (5'-TCAACAGTCACCGACGAGAGTGCTGG-3'); Probe (5′–3′): CGAGTGAAGATCCCCTTTTA. The threshold cycle (Ct) value of each gene was measured and the difference (ΔCt) between target gene and β-GUS (control gene) was calculated. The relative gene expression level was calculated as $2^{(-\Delta Ct)}$.

1.7.5 C-Src *In Vitro* Kinase Assay

201T cells were grown to 80% confluence on 150mm and serum-deprived for 48 h. One plate was stimulated with EGF (50 nM) for 5 min, while another plate was unstimulated. After treatment, cells were lysed in NP-40 lysis buffer, protein concentrations were measured, and equal amounts of protein were subjected to immunoprecipitation. From the EGF-treated cells, total c-Src was immunoprecipitated with the AHO1152 antibody (1 μg) and total c-Met was immunoprecipitated with SC-161 antibody (0.5 μg) from the unstimulated cells overnight at 4°C. These samples were then co-incubated simultaneously with the Protein A-Agarose Beads for 2h at 4°C. Samples were washed 3X with NP-40 lysis buffer, 1X with HNTG Buffer (50 mM HEPES-pH 7.4, 150 mM NaCl, 0.1% Triton X-100, 10% Glycerol), then 1X Kinase Buffer (20 mM HEPES-pH 7.4, 150 mM NaCl, 10% Glycerol, 10 mM $MgCl_2$, 10 mM $MnCl_2$). Samples were resuspended with 1X Kinase buffer and incubated with 0.2 mM ATP for 15 min at 37°C.

After the kinase reaction, 2X Tris-Glycine SDS Sample Buffer was added, samples were boiled, and separated on Tris-Glycine SDS page gels under reducing conditions. Protein was transferred to nitrocellulose membrane and phosphorylated c-Met was assessed by pY99 immunoblotting.

1.7.6 siRNA Transient Transfection

201T cells were transfected with 50 pmol of either c-Met or non-targeting siRNA pools using Oligofectamine (Invitrogen) for 8 h. Transfection medium was replaced overnight followed by experimental treatments.

1.7.7 Analysis of EGF-induced NSCLC Phenotypes

Motility (Wound Healing Assay)

Cells were plated on 12-well plates, grown to a confluent monolayer, and serum-deprived for 24 h. Wounds were created by scraping cells and washed twice with 1X PBS. All treatments were applied every 24 h over the experimental time course. Three wells per experimental treatment were examined 10X magnification by light microscope. Migration distance was assessed by measuring the ability of cells to close the wound area.

Cellular Invasion

Growth Factor Reduced Matrigel-coated Transwell chambers (BD Biosciences) were activated in serum-free media at 37°C for 2 h prior to plating. NSCLC cells ($1x10^4$) were

serum-deprived for 24 h and plated on transwell chambers in 1% charcoal-stripped FBS containing media in the top chamber containing indicated inhibitor treatments. In the bottom chamber, growth factors and inhibitors were refreshed every 24 h. Non-invading cells in the top chamber were removed by cotton swab, and invading cells were fixed and stained using the Diff-Quik staining solutions according to the manufacturer's instructions (VWR International). The number of invading cells was counted at 10X magnification.

Cell Counting Assay

Cells were plated on 6-well plates and allowed to achieve 25% confluence. Plates were serum deprived for 24 h, and all treatments were applied every 24 h. After 48 h, cells were harvested by trypsinization and 8 fields were counted with a hemocytometer at 10X magnification by light microscope. Three wells per experimental treatment were examined.

Clorometric BrdU Cell Proliferation Assay

Cells were played at a density of $1x10^4$ cells per well in a flat-bottom 96-well plate and serum deprived for 24 h. All treatments were applied every 24 h over the 48 h time course. For the final 2 h, BrdU labeling solution was added to each well, cells were fixed, stained with an anti-BrdU antibody, and analyzed in triplicate according to the Clorometric BrdU ELISA manufacturer's instructions (Roche).

1.7.8 Construction of Bioluminescent NSCLC Cell Lines

Construction of pMSCVneo-Luciferase Retroviral Vector

The firefly luciferase gene was cloned from the pGL3 luciferase vector (Promega, Madison, WI) into the pMSCVneo backbone (Clontech, Mountain View, CA) at restriction enzyme sites EcoRI (1406) and BglII (1421) in the multiple cloning site. The primer sequences for cloning were: forward - 5' CGGGAATTCGCCACCATGGAAGACGCCAAAAA-3' and reverse: 5'-GCAGATCTTCATTACACGGCGATCTTTCC-3'.

Production of Luciferase Retrovirus

Luciferase or empty vector retrovirus was produced in Ampho-Pack 293 cells (Clontech) grown in DMEM plus 10% FBS at 37°C, 5% CO2. The vector pMSCVneo-luciferase or pMSCVneo (3 μg) was co-transfected with 3 μg of pAMPHO (Clontech) into Ampho-Pack 293 cells with 3:1 ratio of Fugene (Roche) for 6 h. The growth media was replaced with new full serum medium after 18 h. The following day, the old medium was discarded and replaced with 6 mL fresh DMEM. After 24 hours, the retroviral supernatant was collected and replaced with 6 mL of fresh DMEM. This procedure was continued every 24 h for the next 2 days. All viral pools were combined and stored at -80°C until NSCLC cells were prepared for infection.

NSCLC Infection with Luciferase Retrovirus

201T and A549 cells were grown to 50% confluence in 6-well dishes in full serum medium. The luciferase retroviral media collected from 293 cells was placed on NSCLC cells in the presence of 5 μg/mL polybrene (hexadimethrine bromide). After 4 h, the virus

was removed and replaced with fresh DMEM for 48 h. Cells were split at a 1:4 dilution and individual clones with positive expression of the firefly luciferase was selected for under 600 μg/mL G-418 pressure for 4 weeks.

Luciferase Assay

Luciferase or empty vector clones were grown to 80% confluence on 24-well tissue culture dishes and lysed with Passive Lysis Buffer (Promega). Cell lysates were injected with luciferin substrate and light was measured using the AutoLumat LB953 (Berthold Technologies, Oak Ridge, TN) luminometer. All values are expressed as relative light units.

Implantation of Bioluminescent NSCLC Cells into Nude Mice

Female athymic nude-Foxn1nu 4-5 week old mice were obtained from Harlan (Somerville, NJ) and A549 or 201T NSCLC cells were harvested and suspended in sterile, serum free 1X PBS. The cells were either injected into the hind flank region of each mouse, two sites per mouse (1 $x10^6$ cells per site) or into the lungs via tail vein ($1x10^6$ per mouse). For imaging of bioluminescent cells in vivo, animals were injected with 2oo μL of luciferin substrate into intraperitoneal cavity. Mice were anesthetized with isoflurane, transferred to the imaging platform, and imaged with the Xenogen IVIS Imager (Caliper LifeSciences, Hopkinton, MA) every 7 days for 4 weeks. At the end of the growth period, the animals were sacrificed and lung blocks were removed from selected animals. The lungs were fixed in 10% buffered formalin for gross inspection for

lung tumors. Animal care was in strict compliance with the institutional guidelines established by the University of Pittsburgh.

1.7.9 Evaluation of Combined EGFR and c-Met Therapies in a 201T Xenograft Model of NSCLC

In vivo Tumor Xenograft Model

40 female athymic nude-Foxn1nu 4-5 week old mice were obtained from Harlan (Somerville, NJ) and 201T lung tumor cells were harvested and suspended in sterile, serum free PBS supplemented with 50% Matrigel (BD Biosciences). The cells were then injected in the hind flank region of each mouse, one site per mouse (2 x10^6 cells per site) and allowed to grow to the designated size before administration of compound. Ten days after tumor implantation the mice were divided into 4 treatment groups (10 mice per group): (a) placebo, (b) PF2341066 (c) gefitnib (d) PF2341066 plus gefitnib. Treatment began 10 days after tumor implantation. PF2341066 (50 mg/kg) or vehicle control (0.9% saline/1% Tween-80) was administered daily by oral gavage and gefitnib (150 mg/kg) was administered twice a week by oral gavage. The oral gavage volume was 0.2 mL/mouse and administered for 3 weeks for all treatment groups. Tumor size was measured weekly and reported as an average relative tumor volume calculated as (l *x* w *x* h *x* p)/2 (mm^3), where l is the length, w is the width, and h is the height of the tumor measured with calipers. At the end of the treatment period, the animals were sacrificed and the tumors were removed. Half of the tumor was harvested for protein analysis and

the other half was fixed in 10% buffered formalin for immunohistochemical (IHC) analysis.

Immunohistochemistry

Following antigen retrieval, sections of paraffin-embedded tumors endogenous peroxidase was quenched with 3% H_2O_2 for 10 min, rinsed with deionized water, and washed with TBS buffer before staining. Tumors samples were stained with respective antibodies for 30 min at room temperature then with secondary biotinylated secondary antibody for 25 min at room temperature, followed by streptavidin-conjugated horseradish peroxidase and 3,3′-diaminobenzidine chromogen (Dako, Glostrup, Denmark). Slides were counterstained with hematoxylin for 2 min then dehydrated and cover-slipped.

1.7.10 Statistical Analyses

All values are expressed as the mean ± S.E.M. Student's *t* test was used for all statistical analyses except for the tumor xenograft experiment when an unpaired *t-test* with *Welch's correction* was utilized. Significance tests were performed with a two-sided significance level of 0.05.

2.0 C-MET ACTIVATION BY EGFR IS HGF-INDEPENDENT

2.1 INTRODUCTION

Lung cancer is devastating disease with a 5-year survival rate of 15% largely due to the few effective therapeutic options [1]. Initially, it was hypothesized that treating EGFR-expressing lung tumors with EGFR-targeted therapeutics would prove effective in reducing tumor growth; however, these inhibitors are only successful for the treatment of tumors with activating EGFR mutations, a population that represents only 10% of all NSCLC cases [118]. Lack of clinical efficacy was noted with one major factor being compensatory signaling from the HGF/c-Met pathway in EGFR mutant tumors [42]. Because of these escape pathways, much work is now focused on understanding c-Met and EGFR cross-talk and interactions to identify potential drug combinations to more effectively block tumor progression including the EGFR and c-Met pathways simultaneously. Mediators of cross-talk pathways, especially those receptor tyrosine kinases (RTKs) are ideal candidates due to potential intrinsic resistance through compensatory mechanisms such as what is observed in EGFR and c-Met.

C-Met is frequently co-expressed with EGFR family members in human tumors including NSCLC and it has been demonstrated that these RTKs can signal laterally to one another [75, 78-80]. The mechanisms by which these interactions occur are highly varied. However, one finding spanning the various cell model systems including mutant or overexpressed EGFR is that EGFR activation of c-Met is a rapid event that often

occurs through the formation of transient signaling interactions. Since it is unlikely that c-Met/EGFR heterodimer formation occurs due to lack of SEMA domain homology, there must be additional intermediaries involved with cross-talk. Despite the extensive body of literature documenting EGFR to c-Met cross-talk, these essential mediators have yet to be fully identified, particularly in EGFR wild-type NSCLC cell models that represent approximately 90% of all NSCLC cases.

We previously demonstrated that cellular invasion stimulated by PGE_2 in our NSCLC model system was a delayed event that required EGFR ligand production, c-Met activation, and the Src family kinase (SFK) signaling [88]. Here, we extend our studies to test whether exogenous EGFR ligand stimulation could result in activation of c-Met in NSCLC expressing wild-type EGFR and c-Met receptors with no MET amplification. Further, we aimed to delineate the mechanism and the time course by which this lateral signaling occurs.

2.2 RESULTS

2.2.1 EGFR Ligands Induce Prolonged Phosphorylation of c-Met in NSCLC Cells.

It has been demonstrated that EGFR activation contributes to c-Met tyrosine phosphorylation in a variety of cell models, with varying kinetic parameters [75, 85]. Since NSCLC commonly express both receptors, we examined whether EGFR ligands can induce c-Met phosphorylation in human NSCLC cell lines. 201T and A549 cells were chosen because of moderate expression levels of wild-type EGFR and wild-type c-

Met, which is representative of the majority of NSCLC tumors found in patients (Fig. 7). C-Met is also not altered in these cells as sequencing of c-Met revealed no mutations, and c-Met gene is not amplified in these cell lines (data not shown).

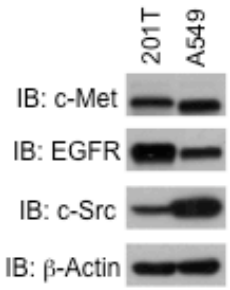

Figure 7. Total c-Met, EGFR, and c-Src expression in NSCLC cell lines. NSCLC cell lines (201T and A549) were analyzed for basal level expression of c-Met, EGFR, and c-Src by whole cell lysate immunoblotting.

Analysis of activated c-Met was performed following stimulation with ligands EGF, TGF-α, or HGF. Time-course analysis of EGF and TGF-α treated 201T cells revealed that c-Met phosphorylation first appears at 8 h and is sustained for 48 h, while EGFR phosphorylation begins at 5 minutes and is completed by 1 h (Fig. 8a and 8b). In contrast, HGF stimulation induced c-Met phosphorylation that begins within 5 minutes and quickly terminates. (Fig. 8a). Similar results were obtained in H1435 and A549 cells (Fig. 8c).

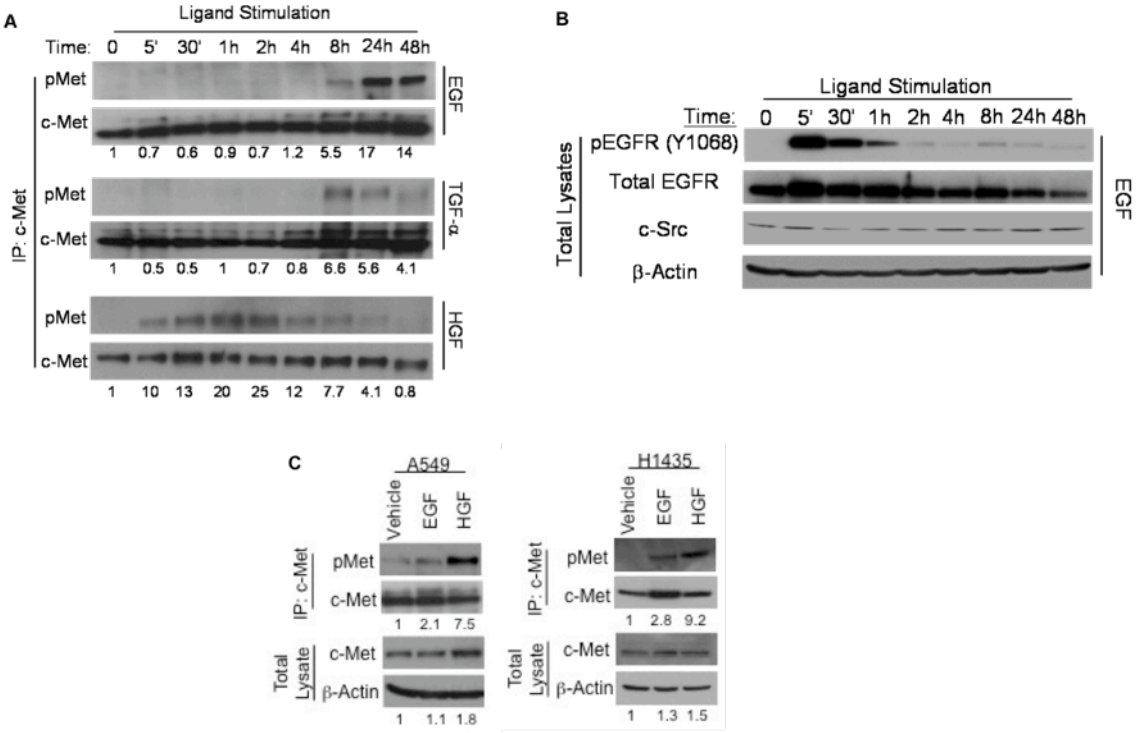

Figure 8. EGFR ligands induce c-Met activation. (A and B) 201T cells were serum-deprived for 2 days prior to stimulation with EGF or TGF-α (10 nM) for 0-48 h or HGF (10 ng/mL) for 5 min. Equal amounts of protein were immunoprecipitated with c-Met and immunoblotted with pY99 and total c-Met antibodies or whole lysates were probed with phospho-EGFR, total EGFR, c-Src, and β-Actin antibodies. (C) A549 and H1435 cells were serum-deprived for 2 days prior to stimulation with EGF (10 nM) for 24 h or HGF (10 ng/mL) for 5 min followed by immunoprecipitation with c-Met and western blotting with pY99, total c-Met, and β-Actin antibodies.

2.2.2 EGFR Ligands Induce c-Met Tyrosine Phosphorylation at Y1003, Y1234/35, Y1349, and Y1365.

The individual c-Met tyrosine residues required for activation and cell signaling are well characterized. The initiating event for c-Met activation is phosphorylation at

residues Y1230/Y1234/Y1235 followed by residues required for cell signaling such as Y1349, Y1365, and Y1003. To determine whether c-Met is being phosphorylated in response to EGFR ligands in a manner similar to that of HGF, we measured individual phospho-tyrosine levels of c-Met. It was confirmed that following EGF stimulation, all tyrosine residues analyzed on c-Met were phosphorylated and followed a pattern similar to HGF stimulation, albeit at delayed time points (Fig. 9a and 9b). Together, these data suggest a novel mode by which EGFR can regulate a prolonged, full activation of c-Met through increased expression levels as well as phosphorylation that persists for long periods.

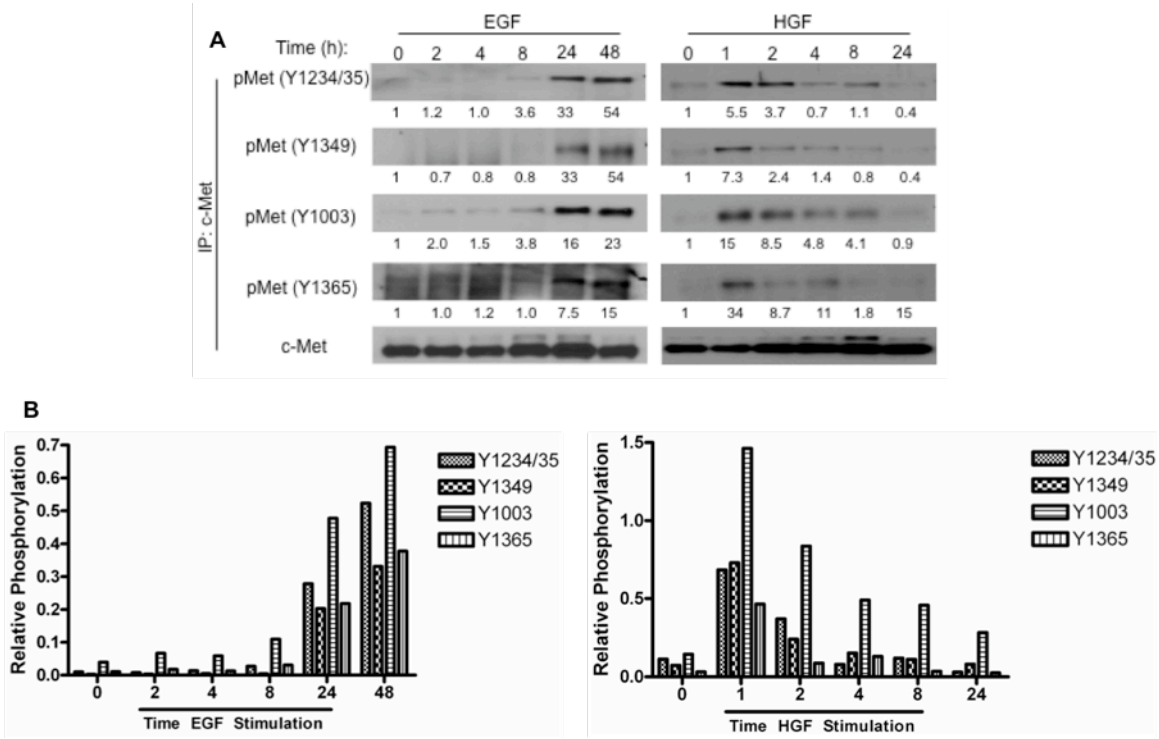

Figure 9. EGF induces specific c-Met tyrosine phosphorylation similar to HGF. (A) 201T cells were serum-deprived for 2 days prior to stimulation with EGF (10 nM) or HGF (10 ng/mL) for 0-48 h followed by immunoprecipitation (IP) with c-Met. Specific c-Met phosphorylation sites were measured by c-Met IP then immunoblotting with phospho-c-Met antibodies: Y1003, Y1234/35, Y1349, and Y1365. All blots were stripped and reprobed with a total c-Met antibody to confirm equal loading. (B) Relative quantitation of c-Met phosphorylation compared to total c-Met protein.

2.2.3 Kinase Activities of Both EGFR and c-Met are Necessary for c-Met Phosphorylation Induced by EGF.

To ascertain the intracellular signaling cascade responsible for c-Met phosphorylation, use of the EGFR tyrosine kinase inhibitor (TKI), gefitinib, was

employed to discern whether EGFR tyrosine kinase activity was required. Pretreatment with gefitinib abolished tyrosine phosphorylation of c-Met induced by EGF, while not inhibiting rapid c-Met tyrosine phosphorylation in response to HGF (Fig. 10a and 10b). These results confirmed that induction of an active EGFR by EGF was needed to facilitate bimodal c-Met activation.

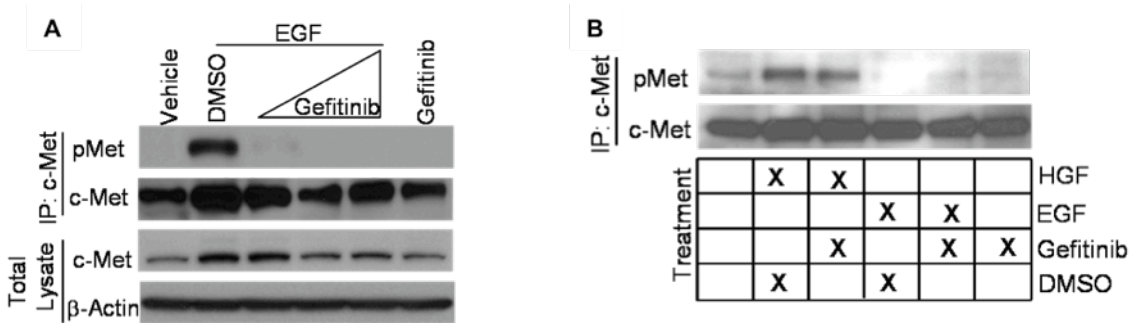

Figure 10. EGFR kinase activity is required for EGF-induced c-Met phosphorylation. 201T cells were serum deprived for 2 days, pretreated with indicated inhibitors, and stimulated with EGF (10 nM) for 24 h or HGF (10 ng/mL) for 5 min. Cell lysates were analyzed for c-Met tyrosine phosphorylation (pY99) and total c-Met. (A) Pretreatment with gefitinib (100 nM, 1 μM, 10 μM) occurred for 2 h, and cells were stimulated with respective ligands. (B) Cells were pretreated with gefitinib (10 μM) followed by stimulation with either HGF (10 ng/mL) or EGF (10 nM) for 5 min. Cell lysates were immunoprecipitated for c-Met and probed for pY99 and total c-Met.

We next addressed whether the kinase activity of c-Met is required for the delayed c-Met phosphorylation. 201T cells were pretreated with selective c-Met TKIs SU11274 and PF2341066 and c-Met phosphorylation status was measured following EGF stimulation (Fig. 11a). These targeted c-Met TKIs had no effect on EGFR autophosphorylation induced by EGF (Fig. 11b). C-Met inhibitors ablated all c-Met

phosphorylation initiated by EGF, while having no effect on c-Met protein up-regulation, demonstrating that c-Met is not being utilized by EGFR as an adaptor-like molecule, but rather delayed activation of c-Met kinase activity is being used to relay the EGFR signal (Fig. 11a).

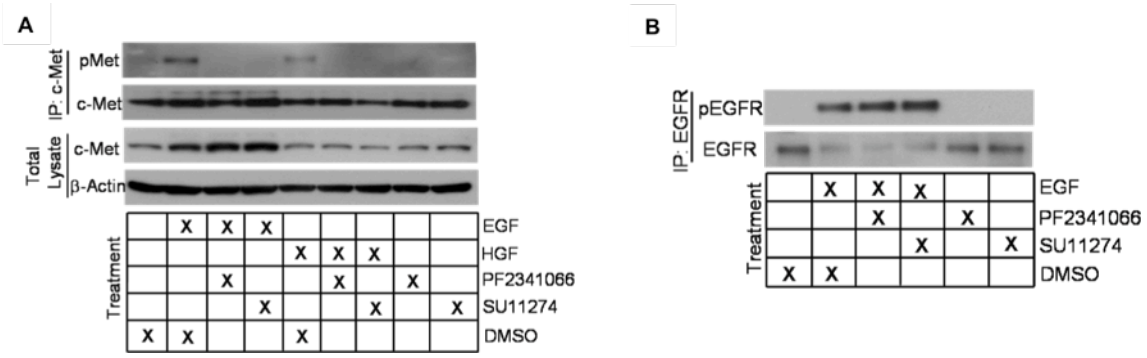

Figure 11. C-Met kinase activity is required for EGF-induced c-Met phosphorylation. 201T cells were serum deprived for 2 days, pretreated with indicated inhibitors, and stimulated with EGF (10 nM) for 24 h or HGF (10 ng/mL) for 5 min. Cell lysates were analyzed for c-Met tyrosine phosphorylation and total c-Met expression. (B) After 2 h pretreatment with the c-Met inhibitors, SU11274 (1 μM) or PF2341066 (1 μM), cells were growth factor treated. (D) 201T cells were pretreated with either SU11274 or PF2341066 (1 μM) followed by stimulation with EGF (10 nM) for 5 min. Cell lysates were immunoprecipitated for EGFR and probed for pY99 and total EGFR.

2.2.4 C-Src is a Key Biphasic Mediator in Signal Transmittance from EGFR to c-Met.

The Src family kinases (SFK) are a group of non-receptor tyrosine kinases including c-Src, which are downstream regulators of tumorigenic phenotypes [119] Members of this family, particularly c-Src, have been identified as key intermediaries in

regulating lateral RTK-RTK signaling [76]. Because of these data and observations of c-Met tyrosine phosphorylation, we hypothesized that the SFKs are critical signaling molecules in delayed EGFR activation of c-Met in NSCLC. To identify the presence of SFK members, we assessed protein expression in the lung cancer cell lines. It was observed that c-Src was ubiquitously expressed across our NSCLC cells with A549 cells expressing the higher level (Fig. 7).

Activation of c-Src is known to be downstream of EGFR [120]. Therefore, we assessed the response to EGF stimulation at delayed time points corresponding with c-Met phosphorylation by measuring levels of activated c-Src in 201T cells. Interestingly, EGF activated c-Src in a biphasic manner (Fig. 12). The initial activation of c-Src was still present 2 h post-EGF stimulation and was subsequently reduced to near baseline levels by 4 h, while the second wave of much greater activation was initiated 8 h post-treatment and lasted 48 h. This pattern of c-Src phosphorylation suggests a temporal association between delayed, persistent c-Src activation and delayed, persistent c-Met activation following EGF stimulation. C-Met may be utilizing c-Src to amplify and prolong signaling from EGFR.

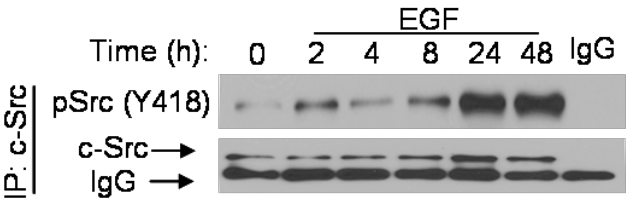

Figure 12. C-Src is phosphorylated at delayed time points. 201T cells were serum deprived for 2 days followed by addition of EGF (10 nM) for 0-48 h. (A) Cell lysates were immunoprecipitated for total c-Src and analyzed for phospho-c-Src (Y418). IgG lane represents immunoprecipitation conditions with only IgG and Protein A Beads without experimental lysate.

We explored whether inhibition of the SFKs could inhibit EGFR-induced c-Met phosphorylation. To address whether c-Src and the SFKs were necessary, pan-SFK inhibitors, PP2 and dasatinib, were employed. A 2 h pretreatment with either PP2 or dasatinib blocked all EGF-induced c-Met phosphorylation while having minimal effect on increased total c-Met protein in response to HGF (Fig. 13a). In contrast, neither PP2 nor dasatinib showed any direct inhibitory effect on c-Met autophosphorylation (Fig. 13b) demonstrating that the SFKs are an intermediary needed for lateral signaling from EGFR to c-Met.

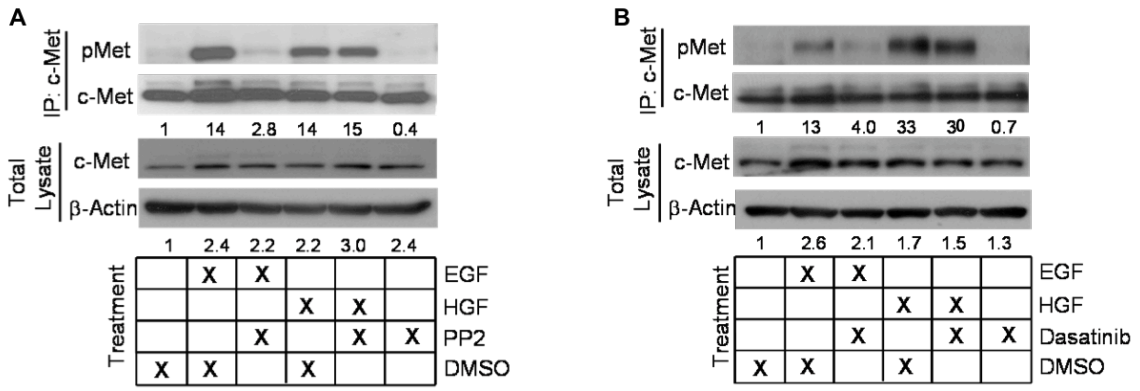

Figure 13. C-Src mediates EGFR-induced c-Met phosphorylation. 201T cells were pretreated for 2 h with SFK inhibitors (A) PP2 (500 nM) or (B) dasatinib (50 nM) prior to 24 h EGF (10 nM) or 5 min HGF (10 ng/mL) stimulation. Cell lysates were prepared and analyzed for phospho- and total c-Met levels.

To discern whether c-Src, specifically, might be the key mediator, 201T cells were stably transfected with either a dominant-negative c-Src construct or an empty vector plasmid as published previously in Liu, *et al* [121]. Stimulation of DN-Src cells for 24 h with EGF resulted in a 2 to 3-fold decrease in total c-Met phosphorylation compared to 201T EV cells (Fig. 14). These experiments advocate that c-Src is a likely candidate molecule that is involved in both initializing EGFR – c-Met trans-activation as well as being a downstream mediator of delayed c-Met activation, although participation of other SFKs in some of the effect cannot be excluded.

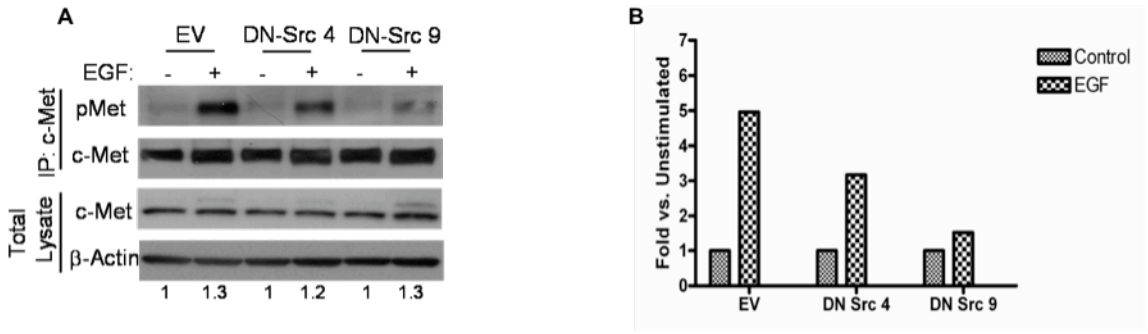

Figure 14. Dominant negative c-Src impedes EGF-induced c-Met phosphorylation. (A) 201T cells were stably transfected with either a dominant-negative c-Src construct (DN-Src) or empty vector (EV), and serum deprived for 2 days followed by addition of EGF (10 nM) for 24 h. Cell lysates were prepared and analyzed for phospho- and total c-Met levels. (B) Relative quantitation of c-Met phosphorylation compared to total c-Met protein.

2.2.5 C-Src Associates with c-Met at time points corresponding with c-Met Activation.

C-Src is activated downstream of c-Met through Src homology-2 domain association with c-Met phospho-tyrosines residues Y1349 or Y1356 following HGF ligand stimulation [59, 120]. We also observed that c-Src was continually activated at later time points. Therefore, we examined whether c-Src could interact with c-Met after exogenous EGF addition. Through co-immunoprecipitation studies following 24 h EGF stimulation, we found that c-Src can associate with activated c-Met in 201T cells suggesting that c-Src activity at 8 h – 48 h time points is mediated downstream of c-Met (Fig. 15).

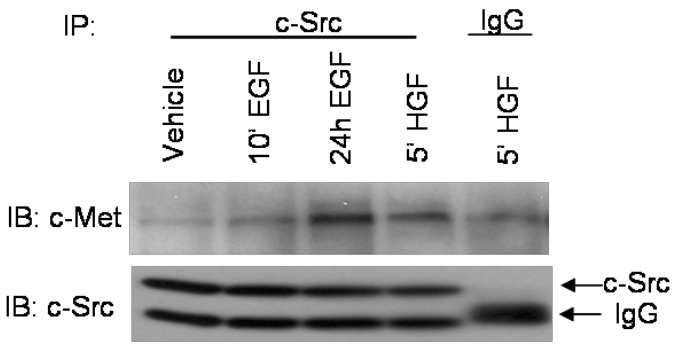

Figure 15. C-Met associates with c-Src following 24 h EGF stimulation. C-Src was immunoprecipitated from EGF (10 nM) or HGF (10 ng/mL) stimulated 201T cells and immunoblotted for total c-Met and total c-Src levels. Non-immune IgG was used as an immunoprecipitation control.

2.2.6 C-Met can be Tyrosine Phosphorylated by c-Src *In Vitro.*

Because c-Src was activated and could associate with c-Met at time points corresponding with c-Met activation, we aimed to determine whether c-Src could directly phosphorylate c-Met. It has been hypothesized that c-Src has the potential to phosphorylate c-Met; however, no direct evidence exists [76]. After a BLAST homology search, it was identified that homology exists between EGFR-Y845, a site known to be phosphorylated by c-Src, and the autophosphorylation site on c-Met, Y1234 (Fig. 16).

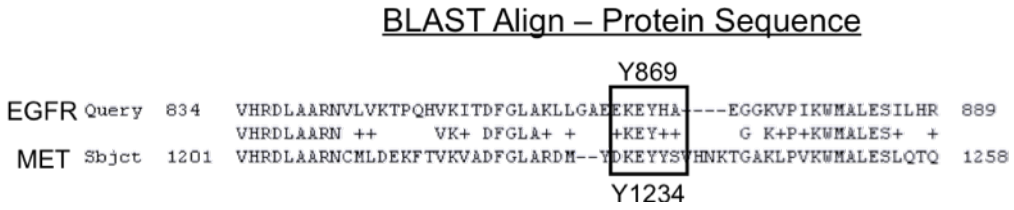

Figure 16. BLAST align search for EGFR and c-Met protein homology.

To test whether c-Src can phosphorylate c-Met *in vitro*, we developed a c-Src kinase assay system utilizing c-Met as a substrate. Total c-Src was immunoprecipitated from 5 min EGF-stimulated 201T cells, while non-activated c-Met was immunoprecipitated from unstimulated 201T cells. The c-Src kinase and c-Met substrate were incubated together with ATP and phosphorylated c-Met was measured through phospho-tyrosine immunoblotting. It was observed that c-Met can be directly phosphorylated by c-Src in the presence of ATP (Fig. 17). This data demonstrates that it is possible that c-Src can directly associate with and phosphorylate c-Met in our signaling paradigm, though subsequent experimentation suggests that a linear signaling cascade directly linking c-Src to c-Met activation is unlikely.

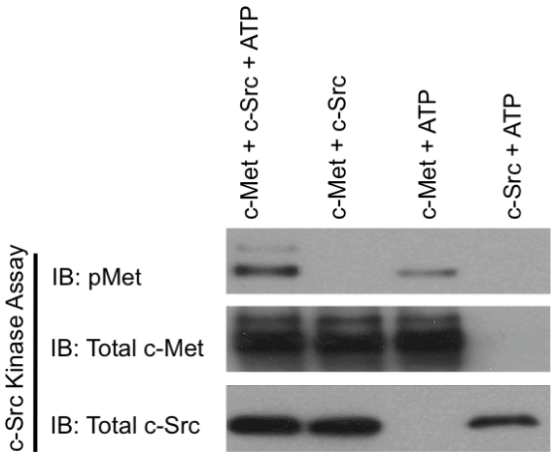

Figure 17. C-Met can be tyrosine phosphorylated by c-Src *in vitro*. 201T cells were stimulated with EGF (50 nM) for 5 min, while another plate was unstimulated. From the EGF-treated cells, total c-Src was immunoprecipitated and total c-Met was immunoprecipitated from the unstimulated cells. These samples were then co-incubated simultaneously with the Protein A-Agarose Beads. Samples were incubated with 0.2 mM ATP for 15 min at 37°C. After the kinase reaction, samples were immunoblotted for phosphorylated c-Met as assessed by pY99 immunoblotting, total c-Met, and total c-Src levels.

2.2.7 Increased c-Met Tyrosine Phosphorylation and Protein through EGFR Requires New Gene Transcription.

EGF-induced c-Met tyrosine phosphorylation proceeds after pronounced 8 h delay. We hypothesized that such a delay was required in order to upregulate a yet identified intermediary in this signaling cascade. To test whether new gene transcription was required, 201T cells were pre-treated with the pan-transcription inhibitor, actinomycin D, prior to EGF administration. Inhibition of transcription abolished delayed

EGF-induced phosphorylation of c-Met, while having no effect on direct activation by HGF (Fig. 18a). This demonstrates that a transcriptional component is required for EGFR trans-phosphorylation of c-Met.

In addition to c-Met tyrosine phosphorylation, we also measured a 1.5-2.5-fold rise ($p<0.0005$) (Fig. 18b and 18c) in total c-Met protein and a corresponding 2-4-fold increase ($p<0.005$) (Fig. 18d) in c-Met transcript levels suggesting that the increase in c-Met protein following EGF addition was a result of new gene transcription. Pretreatment with actinomycin D inhibited the increase in total c-Met protein confirming that the increase in c-Met expression through the EGFR pathway was due to new c-Met transcription (Fig. 18a).

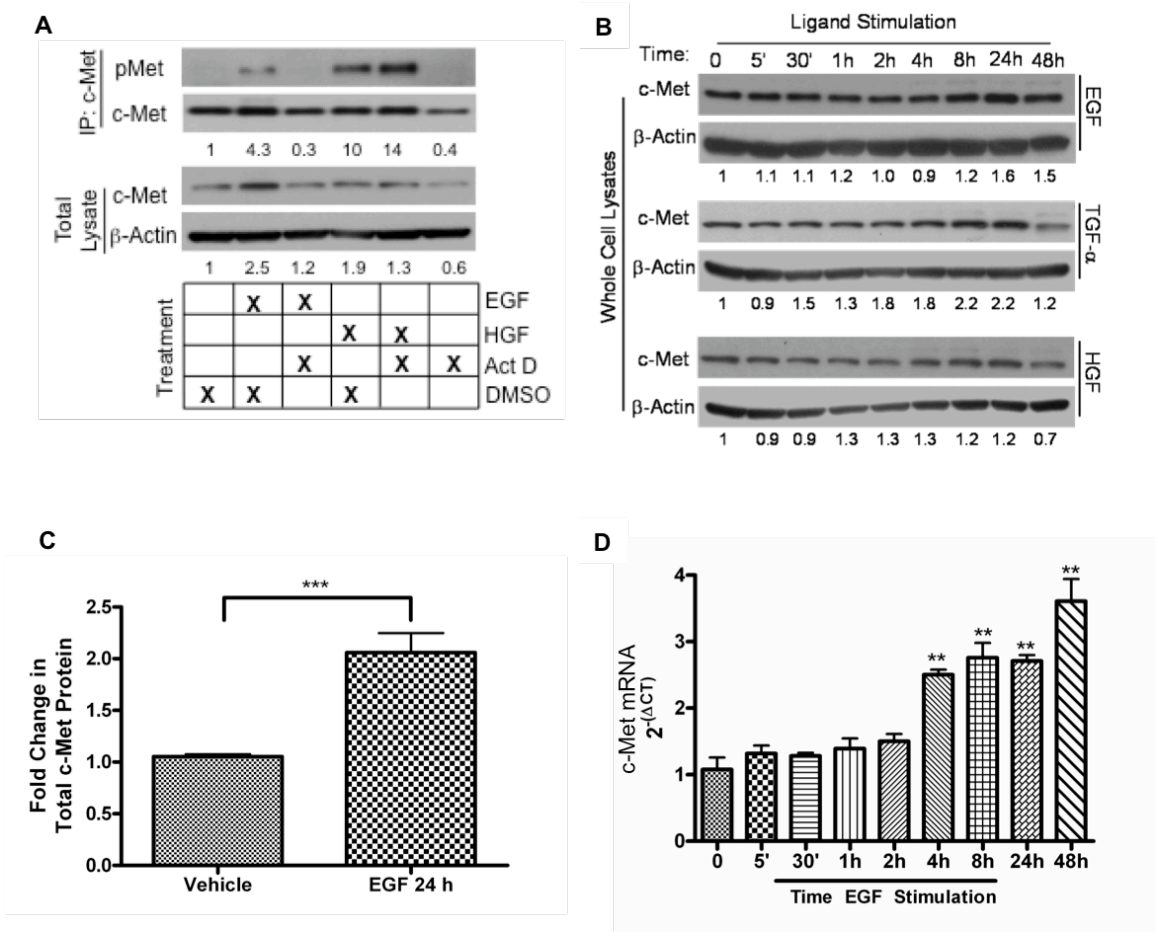

Figure 18. EGF stimulation induces c-Met phosphorylation and increased c-Met mRNA and protein through new gene transcription. (A) 201T cells were serum starved 2 days, pretreated with actinomycin D (0.01 mg/mL), and treated with either EGF (10 nM) for 24 h or HGF (10 ng/mL) for 5 min. Cell lysates were analyzed for c-Met tyrosine phosphorylation and expression. (B) 201T cells were serum-deprived for 2 days prior to stimulation with EGF (10 nM), TGF-α (10 nM), or HGF (10 ng/mL) for 0-48 h followed whole lysate western blotting with total c-Met and β-Actin antibodies. (C) Relative quantitation of total c-Met protein increase compared to β-Actin at 24 h following EGF (10 nM) stimulation in 201T cells. ***, $P < 0.0005$ Student's *t* test. (D) 201T cells were treated with EGF (10 nM) for 0-48 h. Total mRNA was harvested and subjected to c-Met quantitative RT-PCR using β-Gus as an internal control. **, $P < 0.005$ Student's *t* test.

2.2.8 C-Src Inhibition does not Block EGF-Induced c-Met Protein Increase.

It has been hypothesized that c-Met dimerization and activation can result from increased c-Met expression [83, 84]. Because c-Src signaling is critical to EGFR phosphorylation of c-Met, we assayed whether c-Src activation through EGFR was required for elevated c-Met mRNA and protein levels as well. Surprisingly, blockade of c-Src by SFK inhibitor, PP2, had no significant effect on EGF-induced c-Met transcript levels and c-Met protein (Fig. 19). This suggests that c-Src is not upstream of the modest increase in c-Met protein, but may be upstream of other critical transcriptional events regulating c-Met tyrosine phosphorylation.

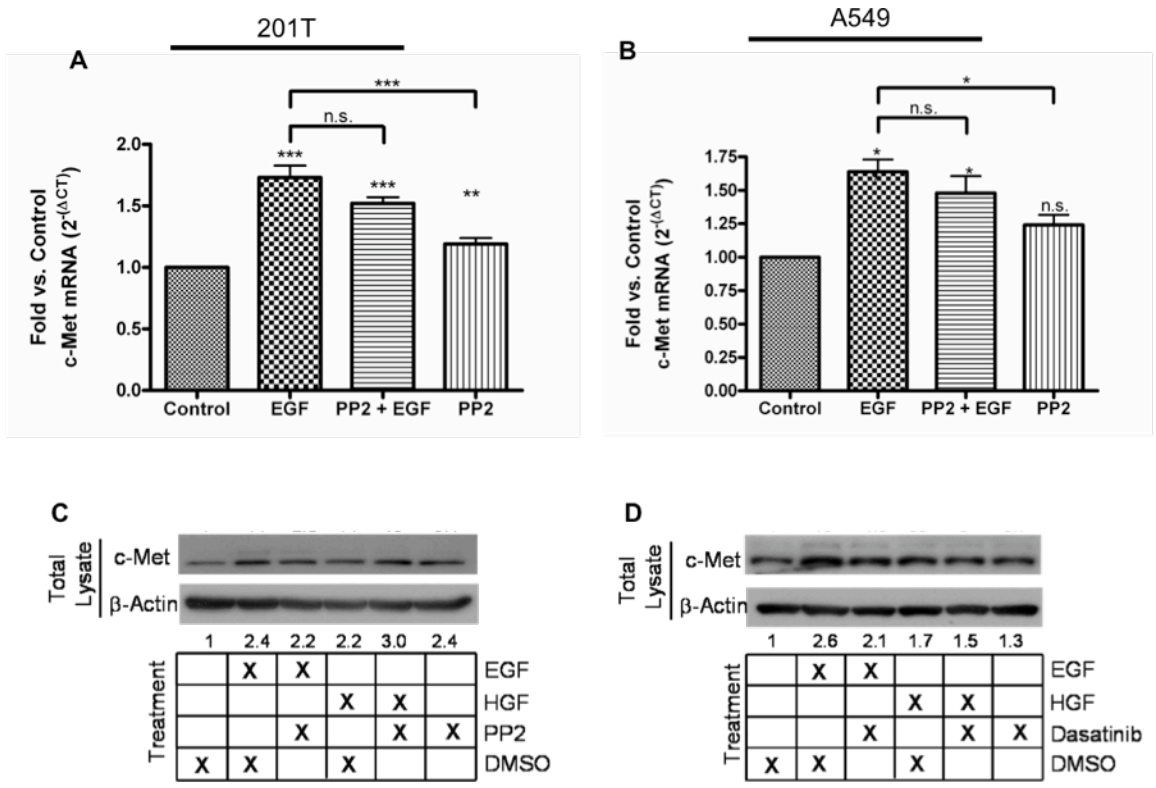

Figure 19. C-Src does not mediate EGFR-induced total c-Met increase. A549 and 201T cells were pretreated for 2 h with PP2 (500 nM) prior to 24 h EGF stimulation. (A and B) mRNA was harvested, and subjected to c-Met quantitative RT-PCR using β-Gus as an internal control. (C) Cell lysates were prepared and analyzed for total c-Met and β-Actin levels. (D) 201T cells were pretreated for 2 h with dasatinib (50 nM) prior to 24 h EGF (10 nM) or 5 min HGF (10 ng/mL) stimulation. Cell lysates were prepared and analyzed for total c-Met and β-Actin levels.

2.2.9 HGF Autocrine Signaling is not Responsible for EGFR-induced c-Met Phosphorylation.

HGF autocrine loops have been observed in many tissue types; therefore, analysis of HGF production and secretion was performed at time points corresponding with c-Met phosphorylation induced by EGF in NSCLC cell lines. 201T and A549 cells were treated with EGF under serum-free conditions and tissue culture media was harvested for HGF ELISA. No HGF secretion was detected in any of the time point samples, suggesting that autocrine signaling is not occurring (Fig. 20a). To confirm this observation, mRNA was harvested from 201T cells following exposure to EGF, and HGF levels were measured. The results from the qRT-PCR assay showed no presence of the HGF transcript produced in unstimulated or stimulated NSCLC cells. (Fig. 20b). A neutralizing antibody to HGF also did not block the EGF-induced phosphorylation of c-Met (Fig. 20c). Based on these data, HGF itself is not involved in the EGF-initiated c-Met lateral signaling.

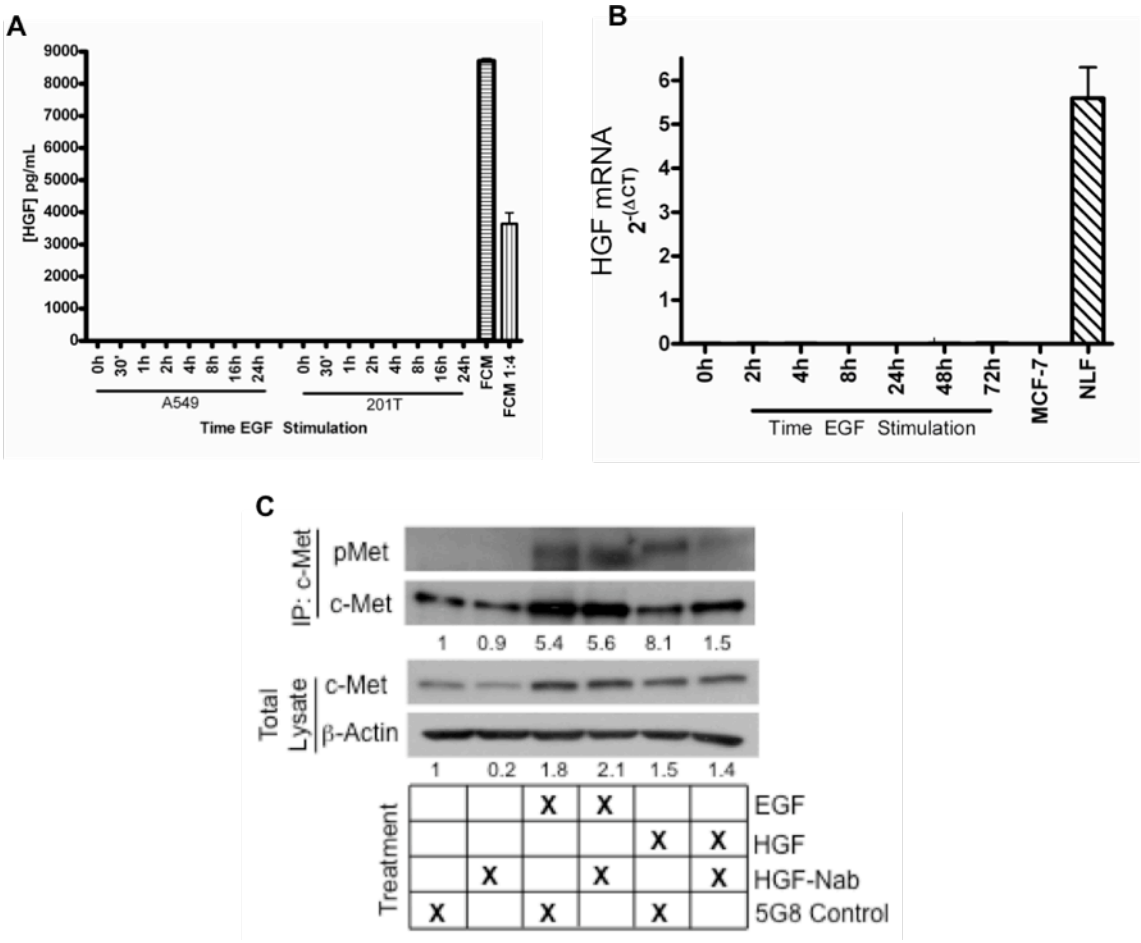

Figure 20. EGFR activation of c-Met does not require HGF production or secretion. A549 and 201T cells were serum starved 2 days prior to stimulation with EGF (10 nM). (A) Tissue culture media was harvested for 0-24 h time points and subjected to HGF ELISA with fibroblast-conditioned media (FCM) as a positive control. (B) Cells were treated, mRNA was harvested, and subjected to HGF quantitative RT-PCR using β-Gus as an internal control. Normal lung fibroblast (NLF) mRNA was utilized as a positive control while the breast cancer cell line, MCF-7, was used as a negative control for HGF expression. (C) EGF (10 nM) or HGF (10 ng/mL) was pretreated for 2 h with HGF neutralizing antibody or IgG control (300 ng/mL) prior to addition to 201T cells for 24 h. Cell lysates were prepared and analyzed for phospho- and total c-Met levels.

2.2.10 The Pathway for Lateral EGFR to c-Met Signaling Does not Require a Secreted Factor.

C-Met is a central molecule that can be activated through various modes of cross-talk signaling from cell surface proteins such as the integrins, RON, RET, plexin B1 as well as others including many G-protein-coupled receptors [77]. In order to begin to uncover other possible intermediates in this signaling cascade from EGFR to c-Met, we measured whether conditioned media from 24 h EGF stimulated 201T cells could induce c-Met phosphorylation of another set of serum-deprived 201T cells. Through whole cell lysate immunoblotting for phospho-c-Met (Y1234/35), phosphorylation of c-Met was identified in the initial 24 h EGF treated cells (Fig. 21 - Lane 9). It was also observed that media harvested from the 24 h EGF-treated 201T cells did not induce c-Met phosphorylation on serum deprived 201T cells up to 48 h (Fig. 21). Taken together, our findings favor an intracellular signaling cascade in the lateral signaling from EGFR to c-Met, and the transcription of an as-yet unidentified protein that is responsible for delayed c-Met phosphorylation.

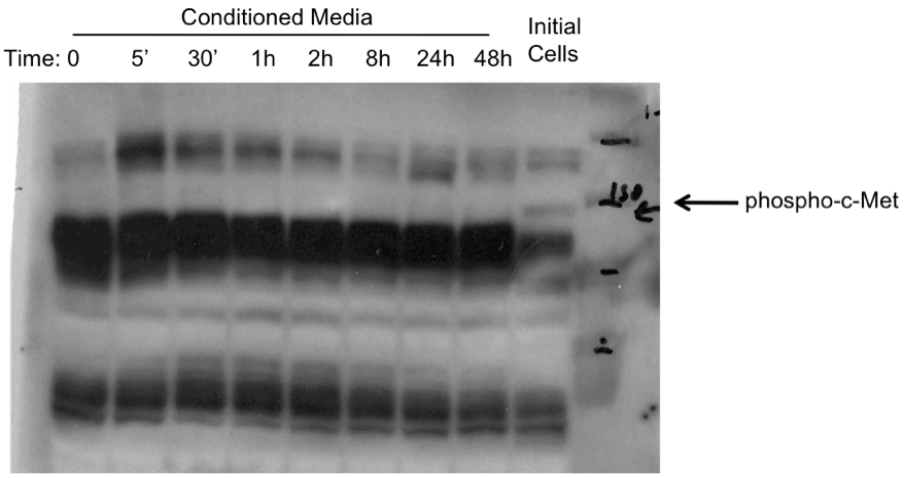

Figure 21. Conditioned media from EGF-treated 201T cells does not induce c-Met phosphorylation. Initial 201T cells were serum starved 2 days prior to stimulation with EGF (10 nM) for 2 h, and the media was replaced with fresh serum free media for an additional 22 h. After the total 24 h, 201T conditioned media was harvested and placed on other serum starved 201T cells for 0-48 h. Whole cell lysates were prepared and analyzed for phospho- and total c-Met levels in both initial cells (lane 8) and conditioned media-treated cells.

2.3 CONCLUSIONS AND DISCUSSION

In these series of experiments, we present findings that the mechanism of lateral communication from EGFR to c-Met relies on a delayed activation of c-Met that is dependent on c-Src. These findings provide an alternative working model of c-Met activation by EGFR in NSCLC cell lines expressing wild-type, non-amplified EGFR and c-Met. Here, EGFR ligands induce prolonged c-Met tyrosine phosphorylation after a pronounced delay that is not attributable to an HGF ligand autocrine pathway. Additionally, we have ruled out the secretion of other factors that might trigger c-Met

phosphorylation because conditioned media experiments could not replicate the EGF-induced effect.

Our results suggest a model for lateral signaling from EGFR to c-Met involving intracellular signaling that is initiated by rapid c-Src activation, requires gene transcription, and leads ultimately to enhanced prolonged c-Src activation that is most likely downstream of c-Met (Fig. 22). While increased c-Met transcription was observed following EGF treatment of NSCLC cells, along with a modest increase in total c-Met protein, this increase in c-Met protein levels appears not to be solely responsible for the delayed c-Met phosphorylation because it is independent of c-Src activity. Based on a recent report, the rise in protein level may be attributed to induction of new c-Met transcripts through EGFR activation of the HIF-1α pathway [85]. Moreover, earlier studies in thyroid carcinoma cells and human gastric carcinoma suggested that increased c-Met levels alone might lead to receptor activation, but concluded that there was a requirement of additional factors to achieve phosphorylation [83, 84]. We hypothesize that after EGFR stimulation, c-Src-dependent transcription of an unknown signaling intermediate accompanies the c-Met increase and is needed for delayed activation of c-Met. Having ruled out secreted factors, the most probable mechanism is the involvement of production of an additional kinase, an inhibitor of a phosphatase, or a scaffolding molecule that could cause ligand-independent c-Met dimerization [122].

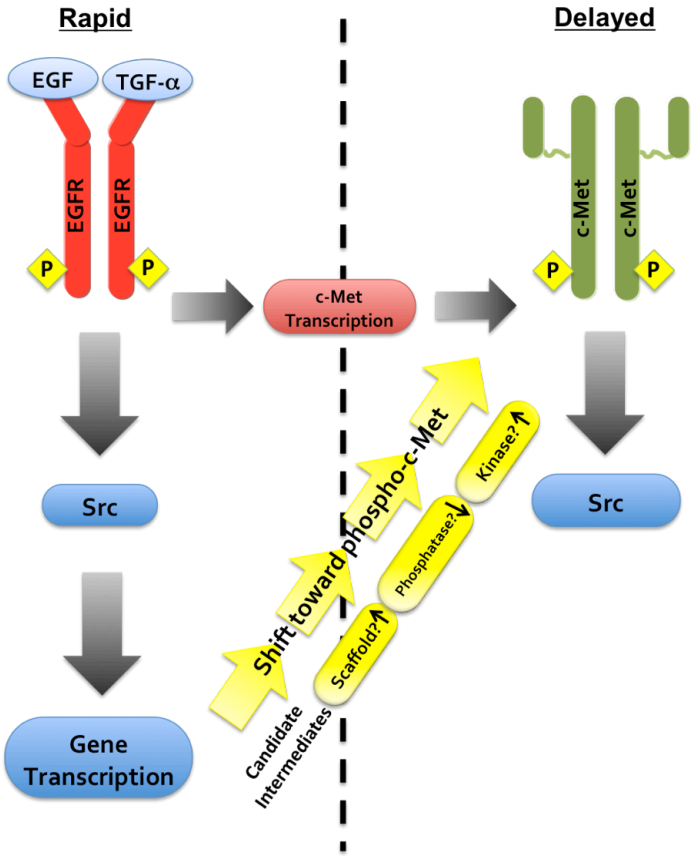

Figure 22. Mechanistic model of EGFR-induced c-Met activation in NSCLC.

C-Src is activated downstream of both EGFR and c-Met following direct ligand stimulation [59, 120]. Here, we showed that delayed c-Src activation is coupled with delayed EGF-induced c-Met phosphorylation, and that c-Src complexes with c-Met at time points after EGF stimulation that correspond to c-Met activation. This occurs when EGFR is no longer activated. The most likely explanation is that c-Src is activated downstream of c-Met through Src homology-2 domains associating with a distinct population of c-Met at phospho-tyrosines residues Y1349 or Y1356 [59]. Although it has been shown that c-Src can signal to HIF-1α, c-Src is minimally involved the pathway we

studied because PP2 had almost no effect on c-Met protein and mRNA levels following EGF stimulation [123]. This suggests that in the NSCLC cell studies, c-Src-dependent c-Met phosphorylation is a distinct event from c-Met upregulation. This is the first time c-Src has been implicated as a critical intermediary linking EGFR activation to c-Met phosphorylation.

It was also measured that c-Src is able to directly phosphorylate c-Met in an *in vitro* model system. Despite this observation, we strongly believe that although this happens in an cell-free kinase assay, it is unlikely that this is applicable to the c-Src role in transmittance of signal from EGFR to c-Met. A large reason for this hypothesis is that c-Src is typically activated in a transient manner, and it is doubtful that c-Src is able to remain activated downstream of EGFR alone for 8 h without a reinforcing loop. Taken together our findings suggest that c-Src initial activation through EGFR initiates a signaling cascade for transcriptional upregulation of a yet-identified intermediate that activates, and sustains, phosphorylation of possibly an intracellular population of c-Met receptors (Early observation). This delayed c-Met activation is then necessary to re-activate c-Src to between 8 h and 48 h to potentially modulate invasive growth phenotypes.

3.0 EGFR PHENOTYPES REQUIRE C-MET

3.1 Introduction

It has been well-documented that both EGFR and c-Met initiate very similar downstream effector molecules in signaling cascades that modulate pathways related to tumor growth and metastasis. The critical pathways have been well documented and include the K-Ras/MAPK, PI3K/AKT, β-catenin/E-cadherin, and STAT pathways amongst many others (Fig. 4). Moreover, many studies have demonstrated that cross-talk amongst pathways can occur particularly to escape receptor blockade. In these cases, the initiating signal for downstream activation is shuttled from one RTK to another as the tumor continues to progress.

Lateral signaling has been identified between c-Met and other molecules including EGFR and RON through varying mechanisms. These studies have implicated lateral activation of c-Met to be required for multiple phenotypes such as cell migration, cellular invasion, angiogenesis, and cell survival [77]. Despite these many studies in a variety of model systems, little is known regarding the impact of delayed and prolonged activation of c-Met through EGFR on known EGF-induced biological outcomes of cell migration, invasion, and proliferation. Based on our observations of delayed c-Met activation by EGF, we hypothesized that c-Met mediates at least part of the EGFR-induced invasion, motility, and proliferation that leads to tumor progression.

3.2 RESULTS

3.2.1 C-Met siRNA Specifically Reduces c-Met Expression in 201T Cells.

In addition to c-Met TKI inhibition with PF2341066, we also aimed to down-regulate c-Met activity using RNAi. The extent of c-Met protein reduction was measured by transient c-Met siRNA transfection. Knockdown of c-Met by siRNA pool resulted in a 92% specific reduction of c-Met compared to the non-targeting siRNA pool, while having no effect on c-Src levels (Fig. 23).

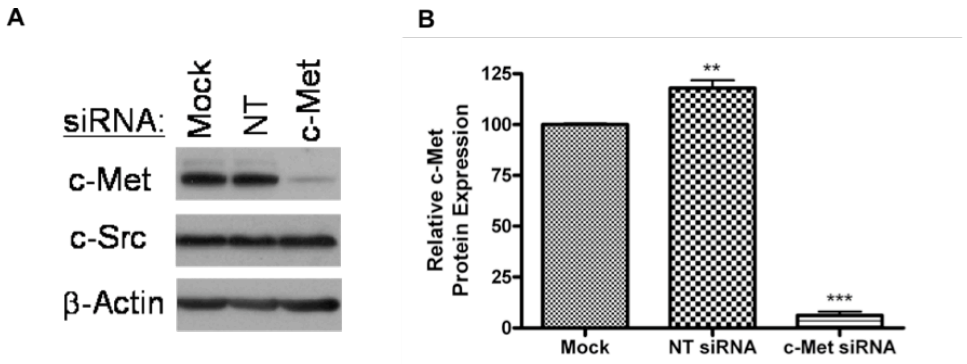

Figure 23. C-Met siRNA specifically decreases c-Met protein levels in 201T cells. 201T cells were mock transfected or treated with either non-targeting siRNA (NT) or c-Met siRNA for 8 h. After 48 h, cell lysates were prepared and analyzed for total c-Met levels, c-Src, and β-Actin. ***, $P < 0.0005$; **, $P < 0.005$ Student's *t* test.

3.2.2 The c-Met Inhibitor, PF2341066, and c-Met siRNA Block EGF-induced NSCLC Cell Invasion

The HGF/c-Met signaling cascade is critical to regulating complex signaling pathways required for cellular invasion; therefore, it was measured whether c-Met was required to mediate the known EGFR phenotypes of invasion. 201T and A549 NSCLC cell lines were pre-treated with the specific c-Met inhibitor, PF2341066 (1 μM), prior to EGF exogenous addition. PF2341066 treatment significantly reduced EGF-induced 201T and A549 cellular invasion by 86% at 48 h. and HGF-induced invasion by 98% in both cell lines (Fig. 24a-c).

To confirm findings that c-Met is required to fully modulate EGF-induced invasion, experiments were repeated with c-Met siRNA. C-Met down-regulation with siRNA resulted in similar results to the PF2341066 at 48 h in EGF-induced invasion experiments, where a 77% reduction in EGF-induced invasion was observed in 201T cells (Fig. 24d). As a control, HGF-induced invasion was inhibited by 86% by siRNA knockdown (Fig. 24d). These findings demonstrate that EGFR requires c-Met to activate the EGFR phenotypes of invasion in NSCLC cell lines.

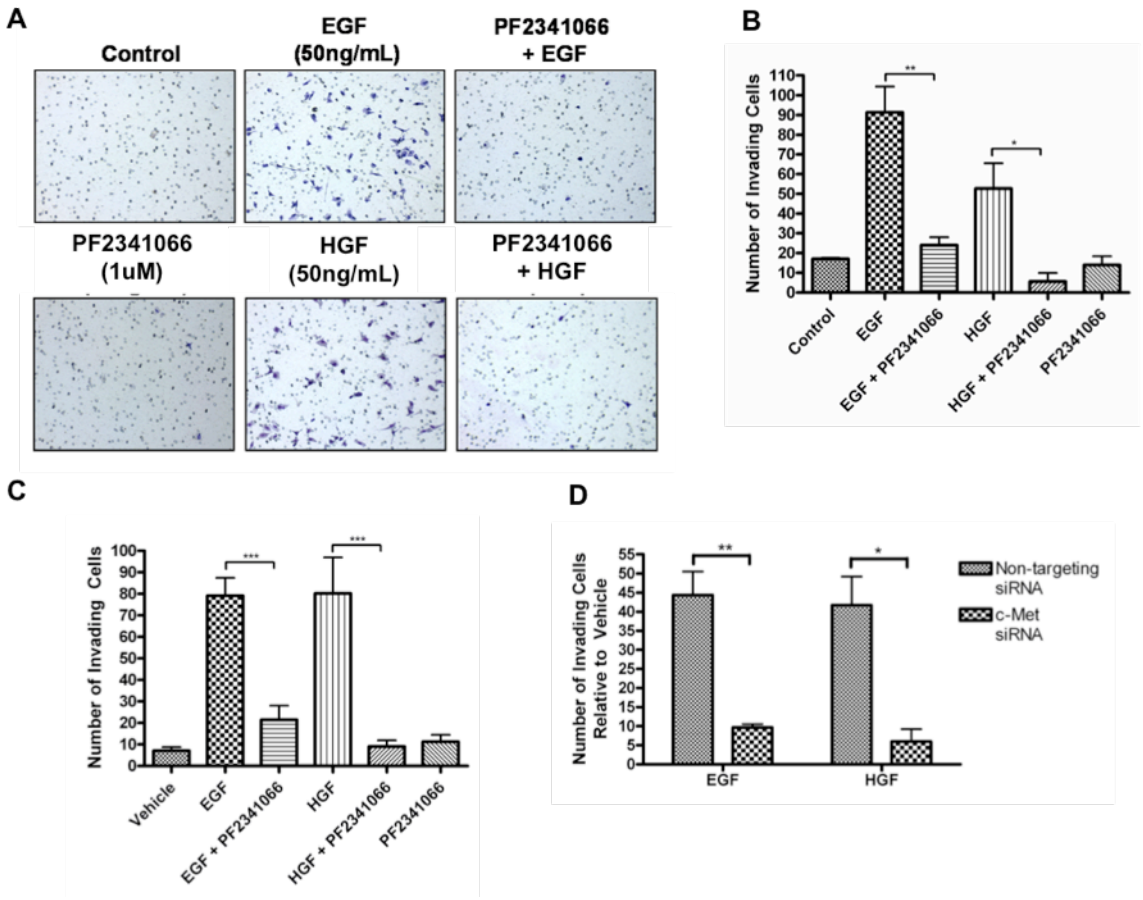

Figure 24. EGFR relies on c-Met for maximal induction of EGFR invasion. Cells were serum deprived for 24 h prior to all 48 h invasion assays stimulated with EGF (50 ng/mL) or HGF (50 ng/mL). For experiments involving PF2341066 (1 μM), cells were pretreated with the c-Met inhibitor or DMSO for 2 h. For c-Met siRNA transfection experiments, 201T cells were plated and subjected to non-targeting siRNA or c-Met siRNA. Following transfection, cells were serum deprived in 24-well Matrigel invasion chambers. 201T (A and B) and A549 cells (C) were plated in Matrigel invasion chambers with growth factors added to the lower chamber only. Invading cells of three independent experiments were counted by light microscopy at 10X magnification. (D) Invasion assays were repeated in 201T cells with c-Met or non-targeting siRNA knockdown as described previously. Mean of three independent samples per treatment group. ***, $P < 0.0005$; **, $P < 0.005$; *, $P < 0.05$ Student's *t* test.

3.2.3 PF2341066 and c-Met siRNA Block NSCLC Cell Migration Initiated through EGFR

In addition to invasion, activation of downstream effector molecules by EGFR and c-Met lead to enhanced cellular migration. Therefore, we assessed whether c-Met was required, in some capacity, for EGF-induced migration. Cell migration initiated through EGFR, as assessed by wound healing assay, was inhibited with PF2341066 by 81% and 57% in 201T and A549 cells, respectively (Fig. 25a-c). As a control, HGF-stimulated migration was inhibited by 95% in 201T cells and 92% in A549 cells (Fig. 25b-c). C-Met down-regulation with siRNA reduced EGF-induced wound healing by 53% in 201T cells (Fig. 25d). HGF stimulated cell migration was inhibited by 86% (Fig. 25d). These experiments substantiate that EGFR, in some capacity, requires c-Met to fully carry out the known phenotype cell motility.

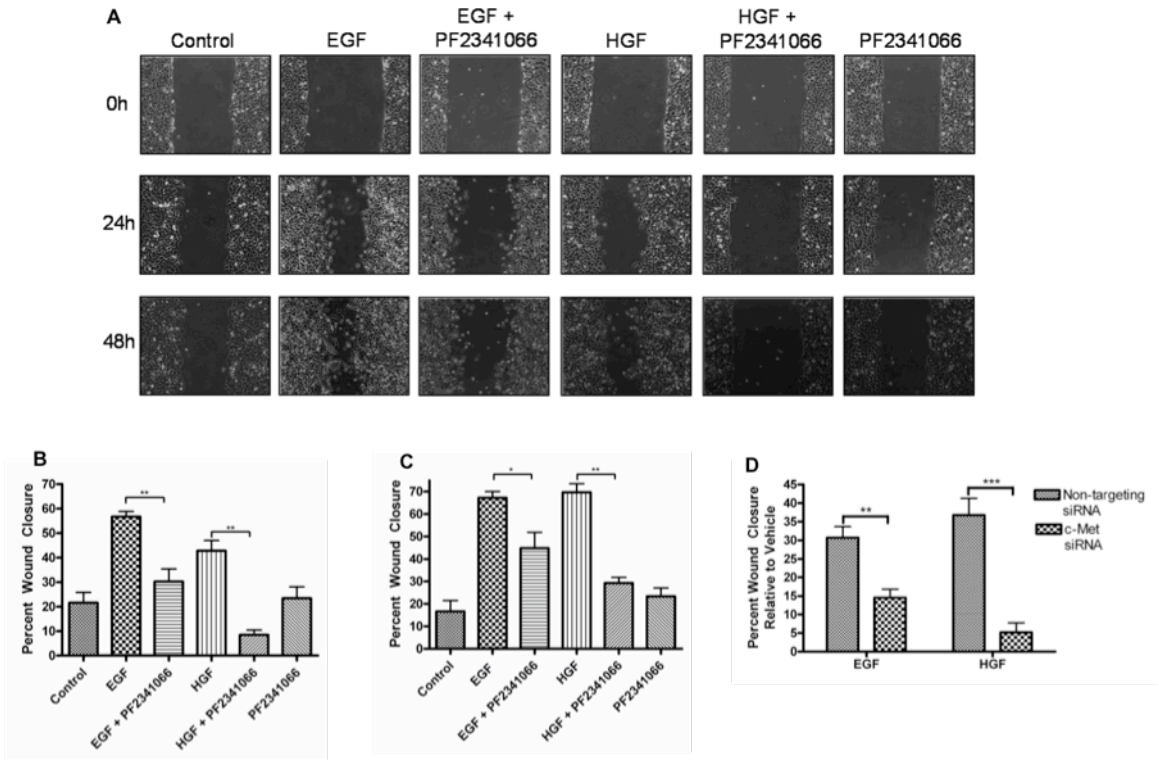

Figure 25. EGFR relies on c-Met for maximal induction of EGFR cell migration. Cells were serum deprived for 24 h prior to all 48 h invasion assays stimulated with EGF (50 ng/mL) or HGF (50 ng/mL). For experiments involving PF2341066 (1 μM), cells were pretreated with the c-Met inhibitor or DMSO for 2 h. For c-Met siRNA transfection experiments, 201T cells were plated and subjected to non-targeting siRNA or c-Met siRNA. Following transfection, cells were serum deprived in 12-well plates for wound healing assays. 201T (A and B) and A549 cells (C) were grown on 12-well plates prior to serum starvation and wounding. Addition of ligands followed c-Met inhibitor pretreatment or siRNA knockdown. Wounds were imaged at 0 and 48 h by 10X light microscopy. Migrating cells were measured by comparing 48 h wound size to initial wound size and expressed as percent wound closure. (D) Would healing assays were repeated in 201T cells with c-Met or non-targeting siRNA knockdown as described previously. Mean of at least three independent samples per treatment group. ***, *P < 0.0005;* **, *P < 0.005;* *, *P < 0.05* Student's *t* test.

3.2.4 C-Met Inhibition has Modulating Effects on Cell Proliferation through EGFR.

EGFR and c-Met are both known to induce cell proliferation in a variety of cell model systems following an activating stimulus. Because we demonstrated that invasion and migration induced through EGFR required c-Met activation, it was hypothesized that EGF-induced cell proliferation required lateral signaling as well. Pre-treatment with the c-Met inhibitor, PF2341066, significantly reduced EGF-induced cell proliferation by 30% in 201T cells and 51% in A549 cells as assessed by cell counting assays. Interestingly, HGF-induced proliferation was only significantly inhibited by 31% in the 201T cell line, although a decreasing trend was observed in the A549 cells, where a 47% reduction was measured (Fig. 26).

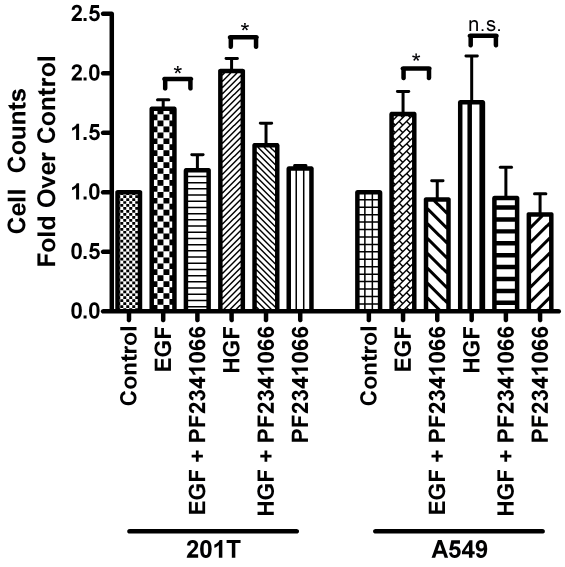

Figure 26. PF2341066 partially inhibits EGF-induced cell growth. 201T and A549 cells were serum deprived for 24 h prior cell counting assays stimulated with EGF (50 ng/mL) or HGF (50 ng/mL). For experiments involving PF2341066 (1 μM), cells were pretreated with the c-Met inhibitor or DMSO for 2 h. After 48 h, cells were harvested by trypsinization and 8 fields were counted with a hemocytometer at 10X magnification by light microscope. Mean of three independent samples per treatment group. *, $P < 0.05$ Student's *t* test.

We attempted to replicate these findings utilizing the c-Met siRNA pool in BrdU incorporation assays measuring the number of proliferating cells. The down-regulation of c-Met compared to non-targeting control decreased EGF-induced proliferation at 48 h as assessed by BrdU assay in 201T cells (Fig. 27). It is interesting to note that EGF addition merely induced a 1.5 fold increase in cell growth in the non-targeting siRNA cells. This is in accordance with previous findings that EGFR wild-type cells expressing at moderate levels are not "addicted" to EGFR activation for cell growth [124]. It is necessary that a

more sensitive EGFR ligand system and further replicates of these cell proliferation experiments be completed before a precise conclusion can be formulated.

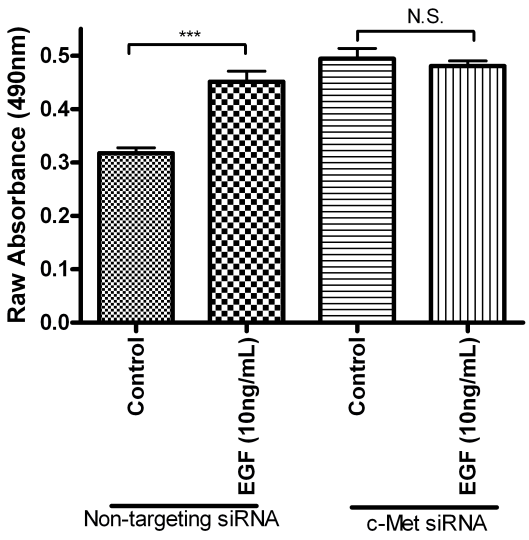

Figure 27. C-Met siRNA knockdown partially inhibits EGF-induced cell proliferation. For c-Met siRNA transfection experiments, 201T cells were plated and subjected to non-targeting siRNA or c-Met siRNA. Following transfection, cells were re-plated and serum deprived in 96-well plates for cell proliferation assays. EGF treatment (50 ng/mL) was applied every 24 h over the 48 h time course. For the final 2 h, BrdU labeling solution was added to each well, cells were fixed, stained with an anti-BrdU antibody, and analyzed in triplicate in a plate reader at 490 nm wavelength.

3.2.5. C-Met Inhibition does not Affect EGF Modulation of pMAPK, pAkt, and E-cadherin

Receptor tyrosine kinase signaling pathways such as those initiated through EGFR and c-Met show a high level of overlap in the activation of key downstream effector molecules such as MAPK (proliferation/migration/invasion), Akt (survival), and

E-cadherin (migration/invasion) (Fig 4). Knowing that EGFR requires c-Met to fully activate some EGFR phenotypes, we assessed whether c-Met was required for modulation of these overlapping effector molecules.

Inhibition of c-Met with PF2341066 was chosen over c-Met siRNA because TKI blockade inhibited all c-Met tyrosine phosphorylation. 201T cells were pre-treated with PF2341066 prior to EGF addition up to 24 h. C-Met targeting had no effect on rapid EGF-induced MAPK, suggesting that the ability of EGFR to initiate this signaling cascade is not affected by status of c-Met (Fig. 28). We also observed that at extended time points (4 h) Akt was not phosphorylated downstream of EGFR. This was anticipated, as c-Met activation does not begin until 8 h following EGF stimulation, whereas MAPK and Akt phosphorylation occur very rapidly (5 min – 1 h) and are returned to basal levels by 24 h (Fig. 28). Moreover, with regard to MAPK signaling, we demonstrated conflicting evidence as to whether c-Met is necessary for EGFR-mediated cell proliferation (Fig. 26 and 27). It would be unlikely this process would occur without MAPK, since this signaling cascade is integral in coordination of cell growth.

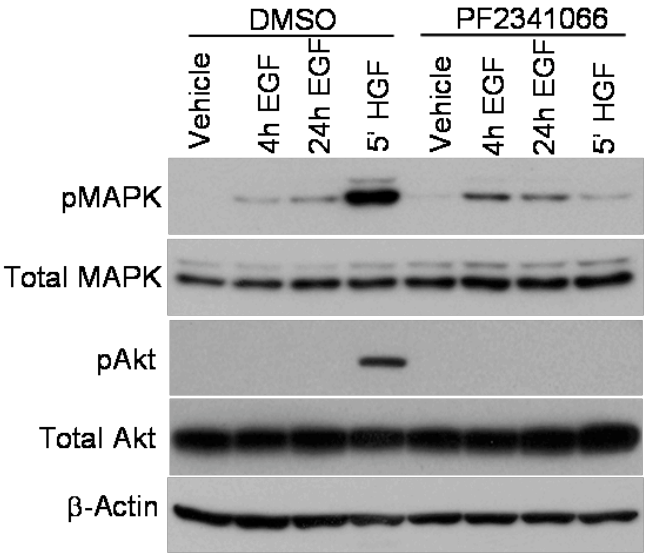

Figure 28. C-Met inhibition has no effect on EGF-induced phospho-MAPK. 201T cells were serum-deprived for 2 days prior to 2 h pretreatment with PF2341066 (1 μM) followed by stimulation with either EGF (10 nM) or HGF (10 ng/mL). Cell lysates were analyzed for MAPK and Akt phosphorylation and expression.

E-cadherin is a cell surface protein that has an important role in cell adhesion. Upon stimuli such as EGFR ligands, E-cadherin is internalized and degraded allowing for cell detachment and cell movement [125]. We measured whether c-Met blockade could impede the down-regulation of E-cadherin following EGF stimulation. It was observed that PF2341066 pre-treatment had no effect on the EGF-induced decrease in E-cadherin at 24 h (Fig. 29).

Despite not identifying a specific molecule requiring lateral signaling to c-Met, pan-phospho-tyrosine immunoblotting of EGF-stimulated 201T cells pre-treated with PF2341066 provided early evidence that a yet-identified protein around 75 kDa requires

EGFR to c-Met signaling (Data not shown). Based on the pattern of migration of this protein, it was hypothesized that this band might represent phosphorylated STAT3.

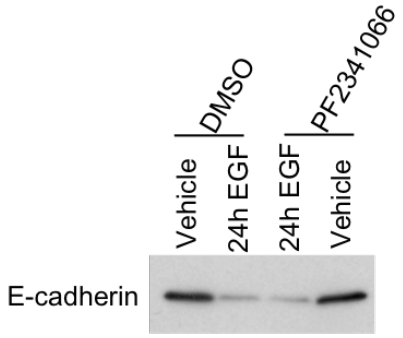

Figure 29. C-Met inhibition has no effect on EGF-modulated E-cadherin. 201T cells were serum-deprived for 2 days prior to 2 h pretreatment with PF2341066 (1 μM) followed by stimulation with either EGF (10 nM). Cell lysates were analyzed for E-cadherin expression.

3.2.6 C-Met is Required for Prolonged STAT3 Activation.

The STAT family of proteins are a group of transcription factors that include STAT3 and are activated downstream of growth factor stimuli including EGF and HGF to upregulate genes related to invasion and cell growth [67, 68]. It was demonstrated that in NIH3T3 and Chang liver cells, HGF stimulation leads to delayed, and prolonged activation of STAT3; therefore, we assessed whether EGF required c-Met to fully induce STAT3 phosphorylation [126]. H1435 cells were pre-treated with PF2341066 prior to EGF addition up to 24 h. C-Met targeting reduced EGF-induced phospho-STAT3 levels to baseline (Fig. 30). This suggests that EGFR requires c-Met to prolong signaling through the STAT3 protein. The requirement of EGFR activation of c-Met to fully activate STAT3 might be necessary for EGF-induced invasion and motility.

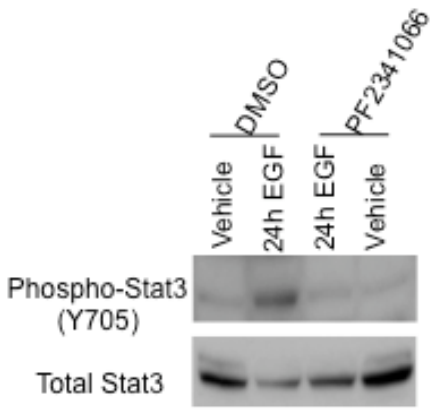

Figure 30. Prolonged STAT3 phosphorylation requires EGFR to c-Met signaling. H1435 cells were serum-deprived for 2 days prior to 2 h pretreatment with PF2341066 (1 μM) followed by stimulation with either EGF (10 nM). Cell lysates were analyzed for STAT3 phosphorylation (Y705) and total expression.

3.3 CONCLUSIONS AND DISCUSSION

Activation of invasion and motility are hallmarks of EGFR signaling that drive lung tumor progression [127]. We showed that EGFR activation of invasive phenotypes relies largely on c-Met signaling through an HGF-independent pathway. A possible explanation is that EGFR utilizes c-Met as a second-in-line molecule not to initiate response, but to amplify the complex phenotypic programs following early activation by EGFR. We also anticipate that an alternative c-Met cascade is being activated at delayed time points, as MAPK and Akt are not phosphorylated at time points corresponding to c-Met phosphorylation. This mode of signaling might occur through intracellular relocalization of a distinct population of c-Met molecules that do not associate with the Gab1 adaptor protein that is known to be required for prolonged MAPK activation [128].

Instead, the observed interaction between c-Met and c-Src, presumably at the c-Met multi-substrate docking site, might preferentially lead to prolonged c-Src activation of regulatory molecules responsible for invasion and cell motility (Fig. 31). It was confirmed that c-Src is integral in these processes as PP2 treatment abolishes c-Src-mediated migration (Data not shown).

Another phenotype associated with EGFR-ligand stimulation leads to increased cell proliferation. Therefore, it was measured as to whether lateral signaling from EGFR to c-Met was required for EGF-induced cell growth. The results from this course of experimentation were varied. One outstanding complexity is the modest increase in cell number or proliferation (1.5-2.5-fold) observed following either EGF or HGF treatment over 48 h. This issue might be attributed to these cell lines expressing only modest levels of wild-type EGFR and non-amplified MET. It is hypothesized that for a certain cell model be "addicted" to a single receptor tyrosine kinase pathway, the receptor levels must exceed a modest level or harbor an activating mutation [124]. Perhaps if we were to utilize, or engineer, a system that had expressed higher concentrations of EGFR, a greater effect on proliferation would be seen with exogenous EGF addition. This, however, would move our research further from the intended model of study. Remaining with our cell model, EGF-induced MAPK phosphorylation was not attenuated by c-Met inhibitors. This was anticipated since MAPK phosphorylation through various stimuli remained up to 24 h, and did not correlate with c-Met activation by EGF. With this observation, we believe that lateral signaling from EGFR to c-Met is unlikely to influence canonical signaling cascades responsible for cell proliferation, as MAPK is a central molecule for this process.

To carry out complex phenotypic alterations through EGFR, precisely coordinated events must be organized at the integration level of effector molecules. We examined whether lateral signaling from EGFR to c-Met modulated levels of phospho-STAT3 and E-cadherin, all of which are highly integral in invasive growth. Of these molecules, prolonged STAT3 phosphorylation appears to be the only molecule identified to date that requires EGFR to c-Met lateral communication. STAT3 activation has been well described in response to EGFR ligand stimulation and is believed to occur through a variety of mechanisms [129]. One particular mode is through direct c-Src and other SFK activation downstream of RTKs that was first described by Cao *et al*. using the v-Src oncogene [130]. The findings described in this study might greatly aid in tying our mechanistic studies described earlier together with the phenotypic responses of invasion, migration, and prolonged STAT3 phosphorylation. We initially hypothesized that activation of c-Met by EGFR is utilized by NSCLC cells to amplify and prolong c-Src signaling. This sustained signal downstream of c-Src would allow STAT3 to also persistently be phosphorylated in homodimer complexes and translocate to the nucleus for transcription upregulation, presumably of genes involved in invasive growth. Additional experimentation of this STAT3 hypothesis is required for specific pathway details; however, we have constructed a strong foundation for future investigations.

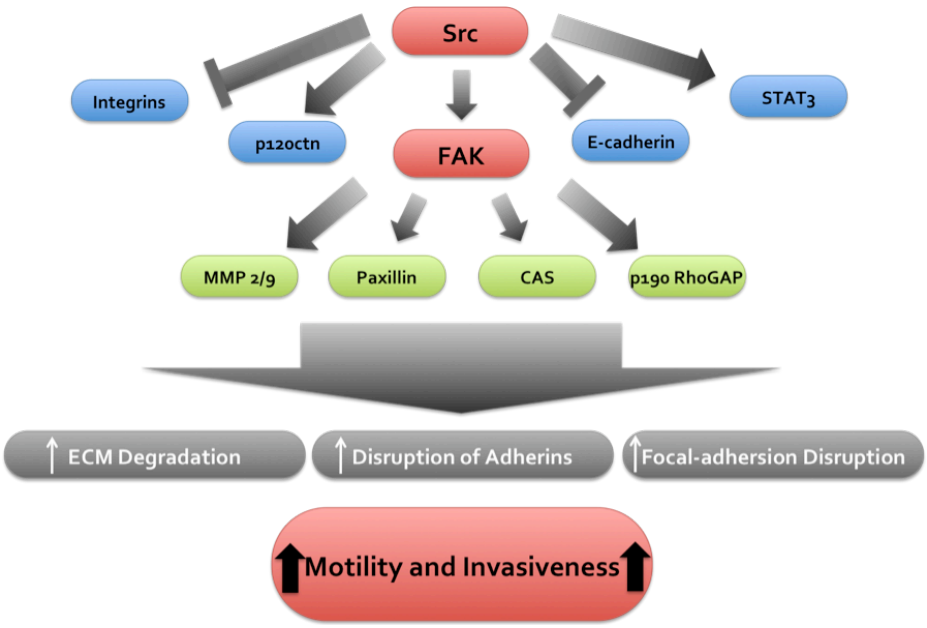

Figure 31. Model of c-Src mediated cell migration and invasion. Adapted from Yeatman, TJ. 2004).

To identify other potential effector molecules regulated by EGFR to c-Met signaling, it appears that a combination of high-throughput techniques such as invasion-focused gene arrays and proteomics, to isolate and identify unknown bands, would be the best course of action. At the point that a additional downstream intermediaries is confirmed, we will have a greater understanding of the manner by which EGFR utilizes delayed and prolonged c-Met activation to regulate EGFR-initiated invasion and motility (Fig. 31).

4.0 COMBINATIONAL TARGETING OF EGFR AND C-MET *IN VIVO*

4.1 INTRODUCTION

There is increasing evidence that c-Met and EGFR signaling pathways interact with one another at multiple cellular levels to circumvent therapeutic inhibition. In particular, Engelman *et al*. established that c-Met signaling is a driver of acquired EGFR tyrosine kinase inhibitors (TKI) resistance in EGFR mutant lung cancer cells and that inhibiting c-Met concurrently could circumvent survival signaling, thus increasing efficacy of EGFR TKIs [42]. Clinical responses to EGFR TKIs in NSCLC patients have produced variable results [131]. In East Asian populations, where there is a high rate of EGFR mutations (~40%), EGFR targeted therapies give a good response. In contrast, patients from western countries tend to have a low frequency of EGFR mutations (3-8% of all lung tumors) and respond poorly to EGFR TKIs [40].

The reason for such low response rates in wild-type EGFR tumors to EGFR TKIs is complex and multi-faceted. In tumors that are initially sensitive to erlotinib and gefitinib, secondary resistance mechanisms emerge following eradication of all sensitive tumors cells. It has been shown that the remaining cells contain a mutant EGFR harboring the EGFR TKI resistant T790M mutation then repopulate the tumor [45-48]. This EGFR mutation renders the tumor cells resistant to EGFR TKIs and confers a proliferative advantage. Primary, or intrinsic, resistance against EGFR therapeutics in lung cancer is associated mutant KRAS expression. These cells are inherently insensitive to many, if not all, RTK targeted therapeutics due to a tumor growth driving force

downstream of RTK activation [43, 44]. Other factors that might be responsible for EGFR TKI resistance is increased ligand production for other RTKs such as the HGF/c-Met pathway allowing shuttling of required downstream signaling to this pathway. To these mechanisms, we include our findings of an intracellular pathway by which EGFR activates c-Met. In utilizing a combined first-line treatment regimen of EGFR and c-Met TKIs, it might be possible to block many of these intrinsic escape mechanisms, and as the tumor becomes resistant to EGFR TKIS, might still provide anti-tumor efficacy through c-Met blockade.

Often ATP-competitive TKIs have off-target effects due to similarly structured ATP binding pockets; however, an inhibitor with cross-reactivity against both EGFR and c-Met has not yet been identified. Therefore, we aimed to determine whether combined TKI therapy of EGFR (gefitinib) and c-Met (PF2341066) provided greater tumor growth inhibition compared to individual therapies in a wild-type EGFR and c-Met model of NSCLC. These experiments were to be initially performed in a 201T xenograft NSCLC model and then utilized in a lung orthotopic, bioluminescent murine model. The bioluminescent orthotopic model was to be created in order to use this combination of targeted agents in a more physiologically relevant environment and to decrease the number of mice utilized for experimentation.

4.2 RESULTS

4.2.1 Combinational Targeting of c-Met and EGFR have Enhanced Anti-tumor Activity in a Xenograft Model of NSCLC.

The identification of delayed c-Met activation in NSCLC cells with wild-type EGFR, as in the case of a majority of NSCLC patients, provides a rationale for combining therapies to improve response to EGFR TKIs. To address whether combinational targeting of EGFR and c-Met pathways leads to enhanced anti-tumor effects, athymic nude mice bearing 201T flank tumors were treated with either gefitinib, PF2341066, combination, or vehicle for 5 d/wk for 3 weeks. PF2341066 alone at a dose of 50 mg/kg had no significant effect on inhibiting tumor xenograft growth, whereas gefitinib significantly reduced tumor volume by 51%. Combining TKI therapies produced a 66% decrease in tumor volume; a significantly greater effect compared to PF2341066 and gefitinib groups, individually (Fig. 32a). EGFR and c-Met targets were confirmed in treatment groups by immunohistochemistry (Fig. 32b). This enhanced effect of EGFR and c-Met combinational therapy observed in this preclinical NSCLC murine model provides early rationale that inhibiting downstream signaling through each RTK as well as lateral signaling might be an effective mode of therapy.

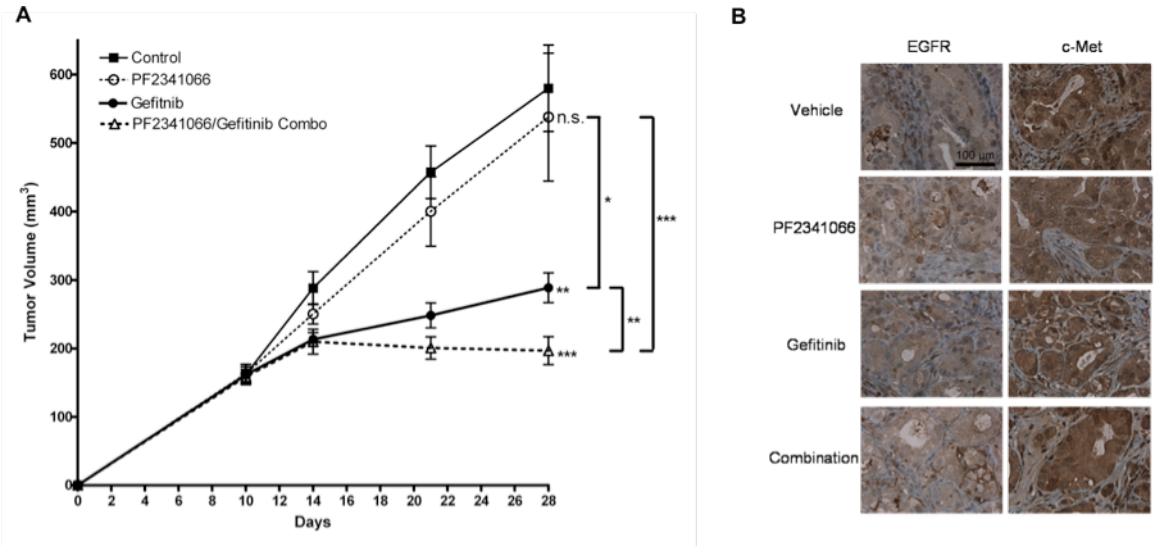

Figure 32. Simultaneous targeting of EGFR and c-Met causes enhanced 201T xenograft tumor growth inhibition. (A) 201T cells ($2x10^6$) were injected into nude mice on day 0. On day 10, tumors were measured and experimental treatments were initiated. PF2341066 (50 mg/kg), gefitinib (150 mg/kg), and vehicle control (0.9% saline/1% Tween-80), were administered daily by oral gavage until day 28. (B) Representative immunohistochemistry of EGFR and c-Met target expression in treated 201T xenograft tumors. Stained tissue sections of xenograft tumors were imaged at 20X magnification. ***, $P < 0.0005$; **, $P < 0.005$; *, $P < 0.05$ Student's *t* test with Welch correction. Everything is compared to the vehicle except where indicated.

4.2.2 Combinational Targeting of c-Met and EGFR have Decreased Ki-67 Staining in Xenograft Tumors.

Measurement of Ki-67 protein levels through immunohistochemistry was performed to identify the extent to which individual or combined treatments inhibited tumor proliferation. Ki-67 staining of xenograft tumors at 28 days revealed significantly fewer proliferating cells in PF2341066 and gefitinib groups individually, while the combination group had a significantly greater effect compared to the individual

treatments confirming the gross measurement of tumor volume (Fig. 33). Additionally, we assessed the number of apoptotic nuclei in 201T xenograft tumors through TUNEL (Terminal deoxynucleotidyl transferase dUTP nick end labeling) staining. No difference was observed through analysis of stained tumor sections (Data not shown).

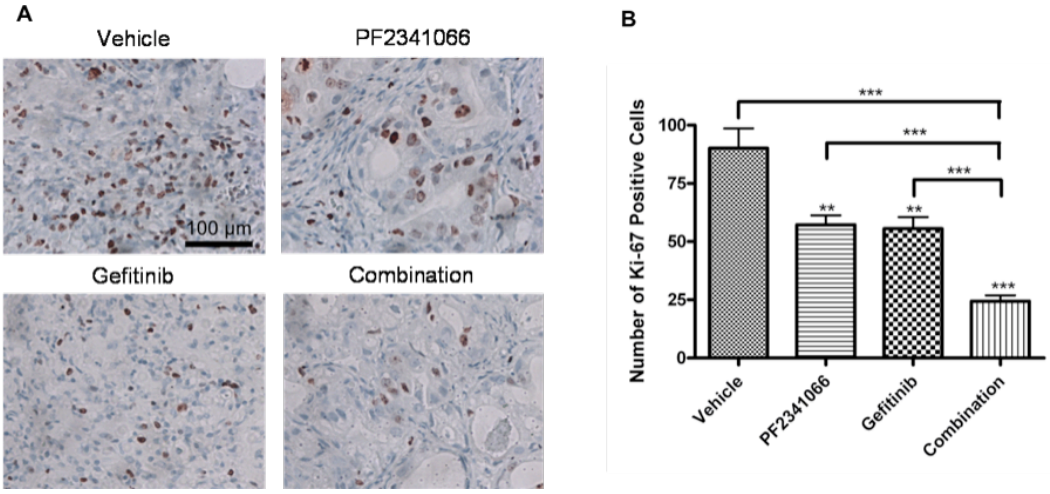

Figure 33. Combinational Targeting of c-Met and EGFR have Decreased Ki-67 Staining in Xenograft Tumors. (A) Representative Ki-67 stained sections of xenograft tumor imaged at 20X magnification. (B) Quantitation of Ki-67 staining was performed by counting 5 fields at 40X magnification. $n = 5$; ***, $P < 0.0005$; **, $P < 0.005$; *, $P < 0.05$ Student's t test. Everything is compared to the vehicle except where indicated.

4.2.3 201T and A549 NSCLC Cell Lines Stably Express Firefly Luciferase.

We then aimed to create a bioluminescent (firefly luciferase), orthotopic model of NSCLC, in which it would be possible to measure EGFR and c-Met combined therapeutic response in a more representative lung tumor environment. The first step in generating this model was to clone the firefly luciferase gene into a vector compatible

with retroviral production. The firefly luciferase gene was sub-cloned from the commercially available pGL3 vector into the pMSCVneo retroviral backbone. Retrovirus was produced and harvested from 293T cells then transduced into the A549 and 201T NSCLC cell lines. Luciferase expression was measured through an *in vitro* luciferase assay, and individual clones (201T- clone 1 and A549- clone 5) expressing the highest level of luciferase selected for implantation into nude mice (Fig. 34).

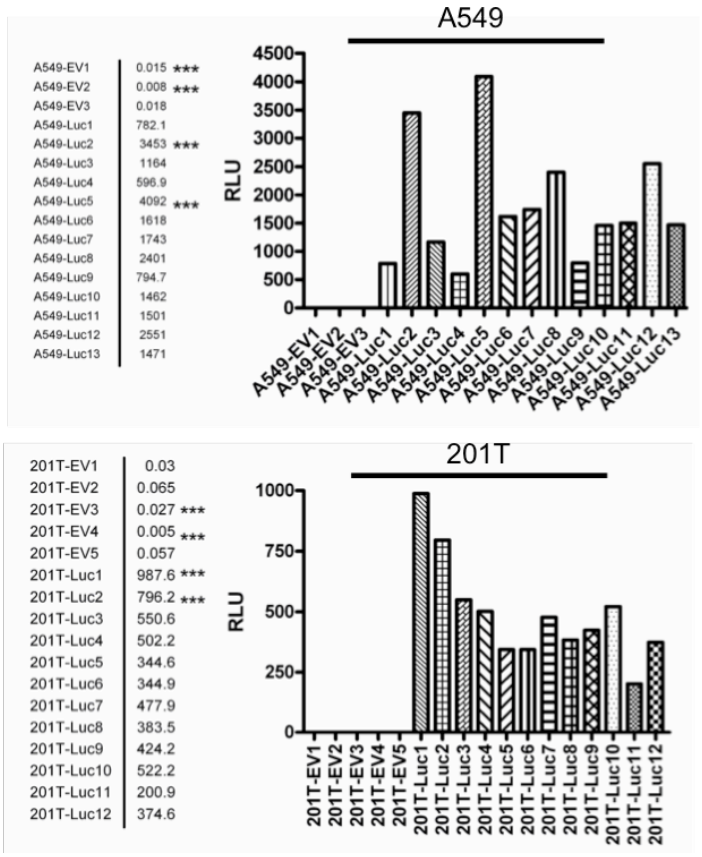

Figure 34. Individual NSCLC cell clones express firefly luciferase. 201T and A549 luciferase or empty vector clones were selected under G-418 pressure for 4 week. Cell lysates were prepared and injected with luciferin substrate. Bioluminescent signals were immediately measured using a luminometer. All values are expressed as relative light units.

4.2.4 201T and A549 Luciferase Cells can be Implanted into the Flank Region of Nude Mice, but not the Lungs.

To test whether the A549 and 201T luciferase cell lines could be detected *in vivo* with the IVIS Xenogen Imager, we implanted A549 and 201T luciferase cells ($1x10^6$) into the flank regions of athymic nude mice. Immediately following subcutaneous injection of the cells, a large cell bolus was observed in both the left (A549) and right (201T) hind regions (Fig. 35). As anticipated, a large percentage of cells died-off 1-week post-injection, but there were small tumors that were still identifiable through imaging. These tumors continued to develop over time until the mice were sacrificed at week 4. The difference in tumor size measured through bioluminescence is probably due to the greater luciferase expression in the A549 cells (4092 R.L.U.) compared to the 201T cells (988 R.L.U.). Ultimately, we demonstrated that both the 201T and A549 luciferase cells could be detected *in vivo* with the Xenogen Imager.

We then tested whether these luciferase NSCLC cells implanted into the lungs could be detected. A549 and 201T luciferase cells ($1x10^6$) were injected via tail vein into the lungs as demonstrated previously [132]. As before with the subcutaneous injection, a large number of luciferase cells were observed in the lungs with a small percentage of the cells being trapped in the tail immediately following injection (Fig. 35). Subsequent measurement of cellular luciferase activity in the lungs, did not register any expression up to 4 weeks post-implantation (Fig. 35). In accordance, gross analysis of lung blocks excised from implanted mice did not reveal tumors in the lungs. We did, however, observe luciferase activity in the tail from trapped cells. These findings suggest that all of

the injected cells in the lungs were destroyed and perhaps more cells need to be injected in the future.

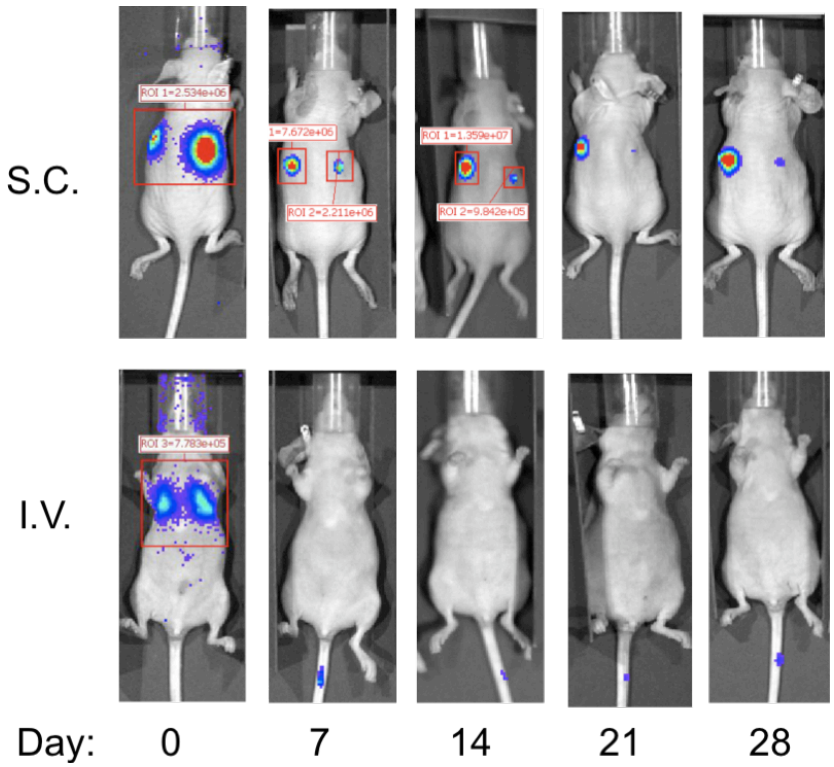

Figure 35. Expression of bioluminescent A549 and 201T cells in nude mice. Luciferase expressing 201T and A549 cells ($1x10^6$) were implanted into nude mice through subcutaneous injection (S.C.) into the hind flank region (left-A549, right-201T) or intravenously (I.V.) into the tail vein on day 0. Mice were and imaged with the Xenogen IVIS Imager every 7 days for 4 weeks. Representative images are shown.

4.3 CONCLUSIONS AND DISCUSSION

In these studies, we focused our efforts on EGFR – c-Met communication in NSCLC cell lines expressing wild-type EGFR and c-Met. Through identification of a

dual-regulation paradigm of tumorigenic signaling from EGFR to c-Met, we further show that combining EGFR and c-Met TKIs provided an enhanced inhibition of tumor growth and a concurrent reduction in Ki-67 staining in 201T xenograft tumors. These results suggest a rationale for simultaneous targeting of EGFR and c-Met to short-circuit signaling cascades responsible for invasive growth initiated and maintained through both receptors as well as trans-activation from EGFR to c-Met.

Early findings established that identification of an over-expressed or hyper-activated molecule in tumor cells might provide an opportunity for specific, single-agent therapy in NSCLC cancer. This observation appears to be true in the case of NSCLC tumors with certain activating EGFR mutations, where these cells are addicted to the EGFR pathway. However, more complex are the tumors that rely on yet-identified molecules or a multitude of input signals to drive cancer progression as the case in the 201T cells that represent of the EGFR and c-Met wild-type model system. It is also important to note that this cell line does not have a K-Ras mutation. To foreshadow the current decision-making process in a clinical setting, this tumor profile would require cytotoxic chemotherapy possibly in combination with EGFR and c-Met TKIs as a first-line treatment. EGFR/c-Met TKI combinations are currently being tested in preclinical and clinical trials in a variety of cancer model systems, and the results appear promising [133-137]. This multiple targeted approach would circumvent some intrinsic mechanisms of resistance as well as delay the emergence of secondary resistance while hopefully decreasing individual dosing levels to decrease toxicity.

In this work, we identified a novel pathway through which EGFR can activate c-Met, thus providing further rationale that this signaling can be an escape mechanism for

both EGFR and c-Met inhibition, individually. Targeting of c-Met and EGFR simultaneously resulted in enhanced tumor growth inhibition, through blockade of downstream signaling from each receptor as well as lateral signaling between EGFR and c-Met to block all tumor growth and potential escape pathways. It would be intriguing to assess the expression of invasion markers such as FAK phosphorylation and MMP expression in this 201T xenograft experiment, or to further utilize a different model to study *in vivo* combination efficacy such as a tumor metastasis model to study disease progression. The rationale behind using this model is due to the requirement of EGFR to c-Met signaling for invasion and migration phenotypes.

We anticipated utilizing this combinational regimen in a bioluminescent, orthotopic model of NSCLC; however, our first efforts were unsuccessful. The 201T and A549 cells were created to stably express the firefly luciferase gene and effectively implanted into the flanks of nude mice where bioluminescence was observed. Unfortunately, despite observed luciferase activity in the lung immediately following injection, it could not be identified at any later time point. This suggests that the entirety of cells were cleared from the lung over time, and not that these cell lines were unable to hone to the lung. In the future, we will increase cell number from $1x10^6$ to identify whether we can get any cells to remain in the lung following implantation.

5.0 DISCUSSION

The main goal of this project was to understand EGFR to c-Met lateral signaling in EGFR and c-Met wild-type NSCLC from mechanistic, phenotypic, and preclinical perspectives to provide rationale for the use of EGFR/c-Met TKI combinations in the clinic. To this end, we demonstrated that there is a dual mode of c-Met activation regulated by EGFR at the post-translational level with tyrosine phosphorylation as well as the expression level with increased total c-Met. The most novel finding is that full c-Met activation occurs 8 h following EGF treatment and is extended up to 48 h due to a requirement of new gene transcription for both phosphorylation and increased c-Met protein. C-Met tyrosine phosphorylation proceeds through an intracellular signaling cascade, where c-Src is critical for EGFR to c-Met signal transmittance. Moreover, c-Src associates with c-Met and is activated at time points corresponding with c-Met activation. We hypothesize that this mode of c-Met activation through EGFR is being utilized to amplify c-Src signaling for known EGFR biological consequences such as invasion and migration through STAT3 phosphorylation. Targeted inhibition of downstream signaling both through c-Met and EGFR as well as lateral signaling to c-Met, enhances tumor growth inhibition in a 201T xenograft model of NSCLC. Taken together, these findings will aid in the future development of combinational EGFR and c-Met TKI treatments in clinical trials for NSCLC tumors with a wild-type EGFR and c-Met profile (Fig. 36).

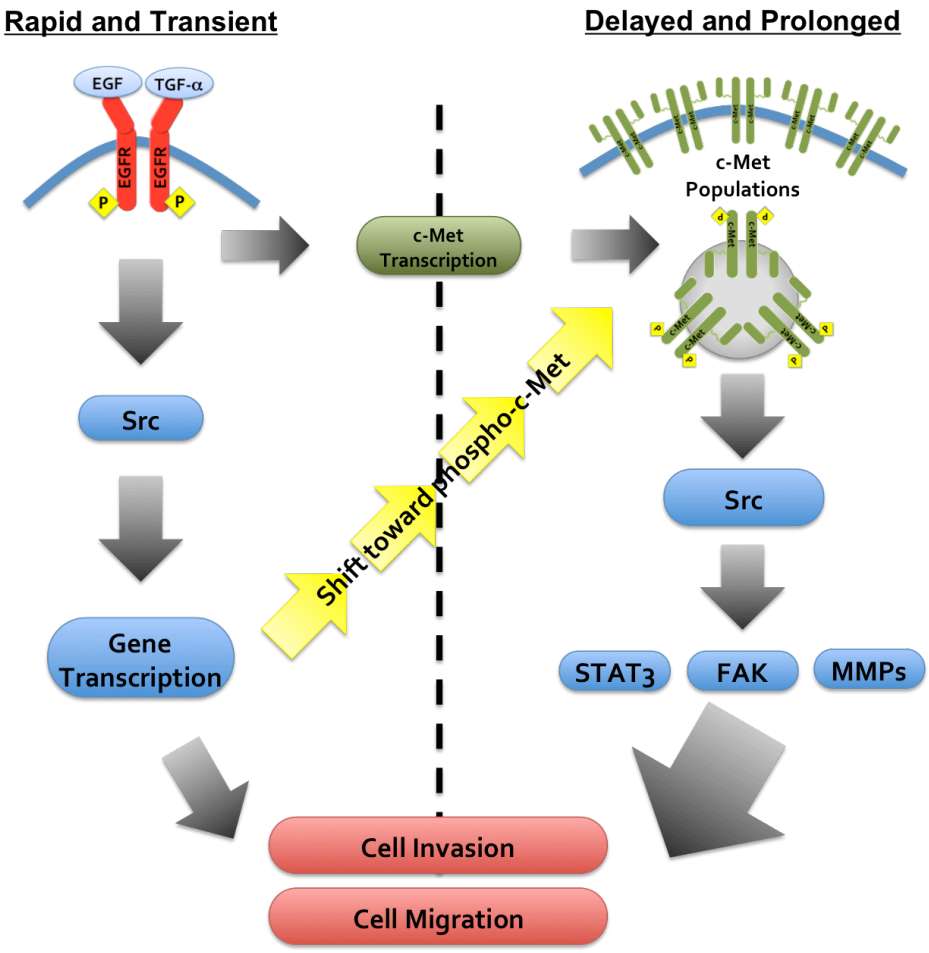

Figure 36. Hypothetical model of EGFR-induced c-Met activation in NSCLC: mechanism and biological consequences.

Defining tumor characteristics through molecular profiling appears to be the future of NSCLC treatment decision-making and has been successful in predicting EGFR TKI sensitivity in EGFR mutant NSCLC tumors. This population, however, is the minority of NSCLC patients. EGFR wild-type tumors represent an overwhelming majority in both North American (90%) and East Asian populations (60%) [40]. Currently, the best available treatment options are cytotoxic chemotherapies such as carboplatin and cisplatin that might increase survival for 1-2 months despite toxic side effects [10-12]. As

the process of detecting driving forces behind this disease is ongoing, it is imperative that we continue to identify future potential agents or combinations to impede NSCLC tumor progression.

One combination study highlights the necessity for targeting multiple RTK inputs in glioblastoma multiforme. These data demonstrate that to completely abrogate survival signaling through the PI3K/Akt pathway, a cocktail of EGFR, c-Met, and PDGFR inhibitors must be employed [138]. This experiment may lend itself well to NSCLC therapy regiments where hyper-activity of EGFR and c-Met are observed clinically. Parallel with these findings, targeted inhibition of downstream effector molecules such as PI3K and MEK might eventually prove to be effective in the treatment of NSCLC [139, 140].

Here, we demonstrate that EGFR and c-Met TKIs combined have a greater effect on blocking pathways responsible for xenograft tumor progression compared to each therapy alone. In this controlled and short exposure environment, we do not expect to observe secondary resistance developments, but in a clinical setting with a more diverse tumor cell population resistance might arise. As combination therapies move forward in the clinic, retrospective analyses should be strongly considered not only to identify sensitive tumors, but to also understand resistance to such therapies.

The identification of EGFR to c-Met lateral signaling that has no extracellular requirement also has important clinical implications in the development of HGF neutralizing antibodies such as L2G7 (Takeda) and AMG 102 (Amgen) [102, 141]. It might be anticipated that in NSCLC tumors with increased production of HGF from the surrounding mesenchymal cells, these targeted inhibitors might be somewhat successful.

However, cells insensitive to this therapy might upregulate EGFR to c-Met signaling to escape HGF neutralizing antibody blockade. Our laboratory is currently involved in preclinical experimentation to combine EGFR TKIs with HGF antibodies, and the early results look very promising (Early observations).

We demonstrated for the first time that c-Src is a key intermediate in EGFR to c-Met activation, which we believe to not be through direct phosphorylation due to signaling kinetics, but rather by transcriptional upregulation of an unknown molecule. As an integral player in tumorigenesis and other cross-talk pathways, c-Src targeted inhibitors have been under therapeutic development [142]. It is of interest to our findings that dasatinib (BMS-354825, brand name Sprycel, Bristol-Myers Squib), a recently approved SFK ATP-competitive inhibitor for melanoma and certain soft tumors, has potent off-target specificity on many RTKs including EGFR [143]. This observation and in conjunction with our mechanistic observations, suggest that combinations of dasatinib with c-Met agents like PF2341066 might prove to be more effective in impeding EGFR and c-Met wild-type NSCLC tumor growth by blocking all three molecules in our identified pathway.

The mechanism involved in EGFR-dependent c-Met activation requires transcription of an unknown mediator that is downstream of c-Src for phosphorylation. Although we showed that the newly transcribed molecule is not HGF or another secreted factor, the exact identity of this protein, or molecule family, remains unknown. It is also strongly believed that this is not due to increased c-Met density resulting in passive phosphorylation. As referenced previously, the other possible scenarios involve the upregulation of either an additional tyrosine kinase, an inhibitor of a phosphatase, or a

scaffolding molecule. In formulating a hypothesis as to the identity of this molecule, one issue that has allowed for little forward movement is the minimal precedence for delayed phosphorylation in general, and no previous data focused on extended c-Met signaling. The theory that we believe to be most plausible is the production of a phosphatase inhibitor. The foundation of this decision is based on empirical findings in addition to process of elimination.

The first possibility is that a produced scaffolding molecule facilitates interaction between two mature c-Met molecules bringing them in close proximity such that trans-autophosphorylation can occur. There is precedence for this mode of signaling that describes the manner by which MAPK cascades function. KSRI is the scaffolding molecule that associates with Raf, MEK, and ERK to relay phosphorylation signals to one another rapidly [144]. In c-Met receptor activation such a mode of activation has not been identified. For this active process to occur with c-Met, a protein or protein complex would have to interact with the intracellular region of each β-chain without interfering with the tyrosine kinase domain or the C-terminus tyrosine residues. For this reason, it seems unlikely that an active c-Met scaffold is being created. An alternative possibility is that there is transcription regulation of a tyrosine kinase molecule.

We initially hypothesized that c-Src could directly phosphorylate and activate c-Met. Experimental evidence demonstrated that this could occur in an *in vitro* system (Fig. 17). However, after many discussions with c-Src "experts", it seems highly unlikely that this transpires in a cellular context. The extended c-Src phosphorylation that we observe might proceed in a biphasic manner following EGF addition (Fig. 12). This early finding suggests that c-Src might be phosphorylated at 2 h, phosphorylation is decreased at 4 h,

and re-emerges at 8 h corresponding with the time point of c-Met activation. If this were entirely upstream of c-Met phosphorylation, this would require EGFR activity to be biphasic or an additional tyrosine kinase to be involved to complete biphasic activation of c-Src. This is not observed following EGF addition (Fig. 8b). Thus, we hypothesize that the late stages of c-Src activation are through the c-Met signaling cascade and not re-activation downstream of EGFR suggesting that c-Src direct phosphorylation of c-Met does not occur. Further experimentation will focus on testing this hypothesis.

If this unknown factor is a different kinase, the overlying question must be addressed, from where does the activating stimulus originate? It is possible that a kinase might be turned on immediately after post-translational processing, but kinases are typically activated in response to stimuli such as direct phosphorylation, dimerization, or binding of multiple protein domains that is observed with adaptor molecules. Additional evidence against an additional tyrosine kinase relies on data demonstrating that phosphorylation of c-Met is prolonged and sustained for up to 48 h after initial EGF stimulation (Fig. 8a and Fig. 9). Kinases without persistent stimulus or activating mutations are often activated in a transient manner to rapidly relay information downstream. In theory, if a kinase was produced as an active molecule, it would be appropriate that an inactivating signal would be quickly initiated. This would suggest that kinase production would also require a coordinating secondary signal to allow prolonged activation.

The most probable scenario is that prior to c-Met phosphorylation, inhibition or down regulation of a protein phosphatase transpires. In a given cell at any time, there is equilibrium of kinase and phosphatase activity ongoing. We believe that to produce such

prolonged c-Met tyrosine phosphorylation downstream of EGFR, the balance of phosphorylation addition and removal is tilted toward increased phosphorylation. For canonical c-Met signaling, phosphorylation is known to be turned off through proteosomal degradation of the c-Met receptor and increased phosphatase activity through interactions as the juxtamembrane region [145]. An interesting note is that these phosphatase molecules have higher affinities for the monomeric form of the c-Met receptor that diminishes as oligomerization occurs [146]. If proven true in our system, then it would be interesting to determine whether c-Met is forming homodimers downstream of EGFR activation as we have illustrated (Fig. 36).

There are existing issues with each of these hypotheses, and it is imperative that much more experimentation be performed in order to focus on other key molecules besides c-Src in this pathway. I believe that in moving forward, the biggest issue lies with the question, "how does direct c-Met phosphorylation occur?" To begin to identify the key molecules required for c-Met phosphorylation, I would suggest a multi-pronged approach. The first step is to identify the pathways and transcription factors activated downstream of EGFR and c-Src activation. This can be performed through literature mining of known transcription factors regulated downstream of c-Src in conjunction with experimentation comparing transcription factor levels of EGF-treated dominant-negative c-Src transfected cells with native NSCLC cells between 4 h and 8 h time points. Once the transcription factors have been narrowed down, further searches can be performed to identify which genes they regulate, and whether these gene products could potentially play a role in c-Met phosphorylation.

To explore this question from an alternate angle, the interacting proteins with c-Met can be assayed through co-immunoprecipitation experiments and mass spectrometry. Based on experimental evidence, it is anticipated that the critical molecule involved in c-Met phosphorylation through EGFR would be interacting with c-Met between 6 h and 8 h following EGF stimulation. This time span would provide a window after new gene transcription through EGFR and just prior to observed c-Met phosphorylation (Fig. 8a). Though there are likely to be many molecules associated with c-Met, the proteins can be further narrowed by comparing EGF- and vehicle-stimulated cells. In utilizing these two methodologies of discovery, candidate molecules will be detected and targeted inhibition and RNAi technologies can be employed to confirm specific involvement in EGFR to c-Met signal transduction.

Based on the body of work presented here, there is still a significant amount of work to be performed in understanding the impact of EGFR initiated c-Met phosphorylation. Our results showed a unique requirement of c-Met to mediate certain known EGFR phenotypes and determined that dual targeting of EGFR and c-Met simultaneously resulted in enhanced anti-tumor effects in a NSCLC xenograft model. Most importantly, we identified a novel pathway by which EGFR can communicate to c-Met through what appears to be an intricate mechanism. These early findings are merely the tip of the iceberg. Further studies should provide exciting insights into the complexities of lateral signaling in NSCLC tumors. It is hoped that the key intermediates in this cascade can be exploited for individual or combinational therapeutic targeting to impede NSCLC progression and ultimately decrease the number of lung cancer deaths.

BIBLIOGRAPHY

1. *American Cancer Society*. http://www.cancer.org/docroot/STT/stt_0.asp, Vol. 1. **Copyright 2008**.
2. Young, R.P., et al., *COPD prevalence is increased in lung cancer, independent of age, sex and smoking history*. Eur Respir J, 2009. **34**(2): p. 380-6.
3. Barnes, P.J., *Chronic obstructive pulmonary disease: effects beyond the lungs*. PLoS Med. **7**(3): p. e1000220.
4. Wingo, P.A., et al., *Annual report to the nation on the status of cancer, 1973-1996, with a special section on lung cancer and tobacco smoking*. J Natl Cancer Inst, 1999. **91**(8): p. 675-90.
5. *Principles & Practice of Lung Cancer*. 4th ed, ed. H.I. Pass, et al. 2010, Philadelpha, PA: Lippincott Williams & Wilkins.
6. Olak, J. and Y. Colson, *Gender differences in lung cancer: have we really come a long way, baby?* J Thorac Cardiovasc Surg, 2004. **128**(3): p. 346-51.
7. Zang, E.A. and E.L. Wynder, *Differences in lung cancer risk between men and women: examination of the evidence*. J Natl Cancer Inst, 1996. **88**(3-4): p. 183-92.
8. Travis, W.D., et al., *Histological typing of lung and pleural tumours*. 3rd ed. 1999, Berlin: Springer-Verlag.
9. Patel, A.M., W.F. Dunn, and V.F. Trastek, *Staging systems of lung cancer*. Mayo Clin Proc, 1993. **68**(5): p. 475-82.

10. Wozniak, A.J., et al., *Randomized trial comparing cisplatin with cisplatin plus vinorelbine in the treatment of advanced non-small-cell lung cancer: a Southwest Oncology Group study*. J Clin Oncol, 1998. **16**(7): p. 2459-65.

11. Gatzemeier, U., et al., *Phase III comparative study of high-dose cisplatin versus a combination of paclitaxel and cisplatin in patients with advanced non-small-cell lung cancer*. J Clin Oncol, 2000. **18**(19): p. 3390-9.

12. Sandler, A.B., et al., *Phase III trial of gemcitabine plus cisplatin versus cisplatin alone in patients with locally advanced or metastatic non-small-cell lung cancer*. J Clin Oncol, 2000. **18**(1): p. 122-30.

13. Kurzrock, R., et al., *Philadelphia chromosome-positive leukemias: from basic mechanisms to molecular therapeutics*. Ann Intern Med, 2003. **138**(10): p. 819-30.

14. *National Comprehensive Cancer Network. NCCN Clinical Practice Guidelines in Oncology: Non-Small Cell Lung Cancer V.1.2010*. 2009 [cited 2010 August 1]; Available from: http://www.nccn.org/professionals/physician_gls/PDF/nscl.pdf.

15. Nicholson, R.I., J.M. Gee, and M.E. Harper, *EGFR and cancer prognosis*. Eur J Cancer, 2001. **37 Suppl 4**: p. S9-15.

16. Laskin, J.J. and A.B. Sandler, *Epidermal growth factor receptor: a promising target in solid tumours*. Cancer Treat Rev, 2004. **30**(1): p. 1-17.

17. Normanno, N., et al., *The role of EGF-related peptides in tumor growth*. Front Biosci, 2001. **6**: p. D685-707.

18. Yarden, Y., *The EGFR family and its ligands in human cancer. signalling mechanisms and therapeutic opportunities*. Eur J Cancer, 2001. **37 Suppl 4**: p. S3-8.

19. Leserer, M., A. Gschwind, and A. Ullrich, *Epidermal growth factor receptor signal transactivation*. IUBMB Life, 2000. **49**(5): p. 405-9.

20. Engelman, J.A. and L.C. Cantley, *The role of the ErbB family members in non-small cell lung cancers sensitive to epidermal growth factor receptor kinase inhibitors*. Clin Cancer Res, 2006. **12**(14 Pt 2): p. 4372s-4376s.

21. Lowenstein, E.J., et al., *The SH2 and SH3 domain-containing protein GRB2 links receptor tyrosine kinases to ras signaling*. Cell, 1992. **70**(3): p. 431-42.

22. Batzer, A.G., et al., *Hierarchy of binding sites for Grb2 and Shc on the epidermal growth factor receptor*. Mol Cell Biol, 1994. **14**(8): p. 5192-201.

23. Chattopadhyay, A., et al., *The role of individual SH2 domains in mediating association of phospholipase C-gamma1 with the activated EGF receptor*. J Biol Chem, 1999. **274**(37): p. 26091-7.

24. Yeatman, T.J., *A renaissance for SRC*. Nat Rev Cancer, 2004. **4**(6): p. 470-80.

25. Leu, T.H. and M.C. Maa, *Functional implication of the interaction between EGF receptor and c-Src*. Front Biosci, 2003. **8**: p. s28-38.

26. Jorissen, R.N., et al., *Epidermal growth factor receptor: mechanisms of activation and signalling*. Exp Cell Res, 2003. **284**(1): p. 31-53.

27. Scaltriti, M. and J. Baselga, *The epidermal growth factor receptor pathway: a model for targeted therapy*. Clin Cancer Res, 2006. **12**(18): p. 5268-72.

28. Van Cutsem, E., et al., *Cetuximab and chemotherapy as initial treatment for metastatic colorectal cancer*. N Engl J Med, 2009. **360**(14): p. 1408-17.

29. Rosell, R., et al., *Randomized phase II study of cetuximab plus cisplatin/vinorelbine compared with cisplatin/vinorelbine alone as first-line therapy in EGFR-expressing advanced non-small-cell lung cancer*. Ann Oncol, 2008. **19**(2): p. 362-9.

30. Kris, M.G., et al., *Efficacy of gefitinib, an inhibitor of the epidermal growth factor receptor tyrosine kinase, in symptomatic patients with non-small cell lung cancer: a randomized trial*. Jama, 2003. **290**(16): p. 2149-58.

31. Fukuoka, M., et al., *Multi-institutional randomized phase II trial of gefitinib for previously treated patients with advanced non-small-cell lung cancer (The IDEAL 1 Trial) [corrected]*. J Clin Oncol, 2003. **21**(12): p. 2237-46.

32. Ciardiello, F., et al., *Antitumor effect and potentiation of cytotoxic drugs activity in human cancer cells by ZD-1839 (Iressa), an epidermal growth factor receptor-selective tyrosine kinase inhibitor*. Clin Cancer Res, 2000. **6**(5): p. 2053-63.

33. Woodburn, J.R., *The epidermal growth factor receptor and its inhibition in cancer therapy*. Pharmacol Ther, 1999. **82**(2-3): p. 241-50.

34. Wakeling, A.E., et al., *ZD1839 (Iressa): an orally active inhibitor of epidermal growth factor signaling with potential for cancer therapy*. Cancer Res, 2002. **62**(20): p. 5749-54.

35. Giaccone, G., et al., *Gefitinib in combination with gemcitabine and cisplatin in advanced non-small-cell lung cancer: a phase III trial--INTACT 1*. J Clin Oncol, 2004. **22**(5): p. 777-84.

36. Herbst, R.S., et al., *Gefitinib in combination with paclitaxel and carboplatin in advanced non-small-cell lung cancer: a phase III trial--INTACT 2*. J Clin Oncol, 2004. **22**(5): p. 785-94.

37. *Tarceva (erlotinib) tablets, oral [package insert]*. . 2009, Melville, NY: OSI Pharmaceuticals Inc.

38. Moyer, J.D., et al., *Induction of apoptosis and cell cycle arrest by CP-358,774, an inhibitor of epidermal growth factor receptor tyrosine kinase*. Cancer Res, 1997. **57**(21): p. 4838-48.

39. Shepherd, F.A., et al., *Erlotinib in previously treated non-small-cell lung cancer*. N Engl J Med, 2005. **353**(2): p. 123-32.

40. Wu, C.C., et al., *Reversed mutation rates of KRAS and EGFR genes in adenocarcinoma of the lung in Taiwan and their implications*. Cancer, 2008. **113**(11): p. 3199-208.

41. Jones, H.E., et al., *Insulin-like growth factor-I receptor signalling and acquired resistance to gefitinib (ZD1839; Iressa) in human breast and prostate cancer cells*. Endocr Relat Cancer, 2004. **11**(4): p. 793-814.

42. Engelman, J.A., et al., *MET amplification leads to gefitinib resistance in lung cancer by activating ERBB3 signaling*. Science, 2007. **316**(5827): p. 1039-43.

43. Eberhard, D.A., et al., *Mutations in the epidermal growth factor receptor and in KRAS are predictive and prognostic indicators in patients with non-small-cell lung cancer treated with chemotherapy alone and in combination with erlotinib*. J Clin Oncol, 2005. **23**(25): p. 5900-9.

44. Gautschi, O., et al., *Origin and prognostic value of circulating KRAS mutations in lung cancer patients*. Cancer Lett, 2007. **254**(2): p. 265-73.

45. Kobayashi, S., et al., *EGFR mutation and resistance of non-small-cell lung cancer to gefitinib*. N Engl J Med, 2005. **352**(8): p. 786-92.

46. Pao, W., et al., *Acquired resistance of lung adenocarcinomas to gefitinib or erlotinib is associated with a second mutation in the EGFR kinase domain*. PLoS Med, 2005. **2**(3): p. e73.

47. Kosaka, T., et al., *Analysis of epidermal growth factor receptor gene mutation in patients with non-small cell lung cancer and acquired resistance to gefitinib*. Clin Cancer Res, 2006. **12**(19): p. 5764-9.

48. Balak, M.N., et al., *Novel D761Y and common secondary T790M mutations in epidermal growth factor receptor-mutant lung adenocarcinomas with acquired resistance to kinase inhibitors*. Clin Cancer Res, 2006. **12**(21): p. 6494-501.

49. Bean, J., et al., *MET amplification occurs with or without T790M mutations in EGFR mutant lung tumors with acquired resistance to gefitinib or erlotinib*. Proc Natl Acad Sci U S A, 2007. **104**(52): p. 20932-7.

50. Nakamura, T., H. Teramoto, and A. Ichihara, *Purification and characterization of a growth factor from rat platelets for mature parenchymal hepatocytes in primary cultures*. Proc Natl Acad Sci U S A, 1986. **83**(17): p. 6489-93.

51. Stoker, M., et al., *Scatter factor is a fibroblast-derived modulator of epithelial cell mobility*. Nature, 1987. **327**(6119): p. 239-42.

52. Mars, W.M., R. Zarnegar, and G.K. Michalopoulos, *Activation of hepatocyte growth factor by the plasminogen activators uPA and tPA*. Am J Pathol, 1993. **143**(3): p. 949-58.

53. Comoglio, P.M., *Structure, biosynthesis and biochemical properties of the HGF receptor in normal and malignant cells*. Exs, 1993. **65**: p. 131-65.

54. Ma, P.C., et al., *c-Met: structure, functions and potential for therapeutic inhibition*. Cancer Metastasis Rev, 2003. **22**(4): p. 309-25.

55. Bottaro, D.P., et al., *Identification of the hepatocyte growth factor receptor as the c-met proto-oncogene product*. Science, 1991. **251**(4995): p. 802-4.

56. Naldini, L., et al., *Scatter factor and hepatocyte growth factor are indistinguishable ligands for the MET receptor*. Embo J, 1991. **10**(10): p. 2867-78.

57. Naldini, L., et al., *The tyrosine kinase encoded by the MET proto-oncogene is activated by autophosphorylation*. Mol Cell Biol, 1991. **11**(4): p. 1793-803.

58. Naldini, L., et al., *Hepatocyte growth factor (HGF) stimulates the tyrosine kinase activity of the receptor encoded by the proto-oncogene c-MET*. Oncogene, 1991. **6**(4): p. 501-4.

59. Ponzetto, C., et al., *A multifunctional docking site mediates signaling and transformation by the hepatocyte growth factor/scatter factor receptor family*. Cell, 1994. **77**(2): p. 261-71.

60. Peschard, P., et al., *Mutation of the c-Cbl TKB domain binding site on the Met receptor tyrosine kinase converts it into a transforming protein*. Mol Cell, 2001. **8**(5): p. 995-1004.

61. Comoglio, P.M. and C. Boccaccio, *Scatter factors and invasive growth*. Semin Cancer Biol, 2001. **11**(2): p. 153-65.

62. Meloche, S. and J. Pouyssegur, *The ERK1/2 mitogen-activated protein kinase pathway as a master regulator of the G1- to S-phase transition*. Oncogene, 2007. **26**(22): p. 3227-39.

63. Maulik, G., et al., *Role of the hepatocyte growth factor receptor, c-Met, in oncogenesis and potential for therapeutic inhibition*. Cytokine Growth Factor Rev, 2002. **13**(1): p. 41-59.

64. Zeng, Q., et al., *Hepatocyte growth factor inhibits anoikis in head and neck squamous cell carcinoma cells by activation of ERK and Akt signaling independent of NFkappa B*. J Biol Chem, 2002. **277**(28): p. 25203-8.

65. Xiao, G.H., et al., *Anti-apoptotic signaling by hepatocyte growth factor/Met via the phosphatidylinositol 3-kinase/Akt and mitogen-activated protein kinase pathways*. Proc Natl Acad Sci U S A, 2001. **98**(1): p. 247-52.

66. Dong, G., et al., *Hepatocyte growth factor/scatter factor-induced activation of MEK and PI3K signal pathways contributes to expression of proangiogenic cytokines interleukin-8 and vascular endothelial growth factor in head and neck squamous cell carcinoma*. Cancer Res, 2001. **61**(15): p. 5911-8.

67. Rivat, C., et al., *Disruption of STAT3 signaling leads to tumor cell invasion through alterations of homotypic cell-cell adhesion complexes*. Oncogene, 2004. **23**(19): p. 3317-27.

68. Song, J.I. and J.R. Grandis, *STAT signaling in head and neck cancer*. Oncogene, 2000. **19**(21): p. 2489-95.

69. Wang, R., R. Kobayashi, and J.M. Bishop, *Cellular adherence elicits ligand-independent activation of the Met cell-surface receptor*. Proc Natl Acad Sci U S A, 1996. **93**(16): p. 8425-30.

70. Nakamura, Y., et al., *Constitutive activation of c-Met is correlated with c-Met overexpression and dependent on cell-matrix adhesion in lung adenocarcinoma cell lines*. Cancer Sci, 2008. **99**(1): p. 14-22.

71. Liu, Y., et al., *Coordinate integrin and c-Met signaling regulate Wnt gene expression during epithelial morphogenesis*. Development, 2009. **136**(5): p. 843-53.

72. Trusolino, L., A. Bertotti, and P.M. Comoglio, *A signaling adapter function for alpha6beta4 integrin in the control of HGF-dependent invasive growth*. Cell, 2001. **107**(5): p. 643-54.

73. Orian-Rousseau, V., et al., *CD44 is required for two consecutive steps in HGF/c-Met signaling*. Genes Dev, 2002. **16**(23): p. 3074-86.

74. Orian-Rousseau, V., et al., *Hepatocyte growth factor-induced Ras activation requires ERM proteins linked to both CD44v6 and F-actin*. Mol Biol Cell, 2007. **18**(1): p. 76-83.

75. Fischer, O.M., et al., *Reactive oxygen species mediate Met receptor transactivation by G protein-coupled receptors and the epidermal growth factor receptor in human carcinoma cells*. J Biol Chem, 2004. **279**(28): p. 28970-8.

76. Popsueva, A., et al., *GDNF promotes tubulogenesis of GFRalpha1-expressing MDCK cells by Src-mediated phosphorylation of Met receptor tyrosine kinase*. J Cell Biol, 2003. **161**(1): p. 119-29.

77. Lai, A.Z., J.V. Abella, and M. Park, *Crosstalk in Met receptor oncogenesis*. Trends Cell Biol, 2009. **19**(10): p. 542-51.

78. Jo, M., et al., *Cross-talk between epidermal growth factor receptor and c-Met signal pathways in transformed cells*. J Biol Chem, 2000. **275**(12): p. 8806-11.

79. Nakajima, M., et al., *The prognostic significance of amplification and overexpression of c-met and c-erb B-2 in human gastric carcinomas*. Cancer, 1999. **85**(9): p. 1894-902.

80. Shattuck, D.L., et al., *Met receptor contributes to trastuzumab resistance of Her2-overexpressing breast cancer cells*. Cancer Res, 2008. **68**(5): p. 1471-7.

81. Presnell, S.C., et al., *Modifications of the hepatocyte growth factor/c-met pathway by constitutive expression of transforming growth factor-alpha in rat liver epithelial cells*. Mol Carcinog, 1997. **18**(4): p. 244-55.

82. Guo, A., et al., *Signaling networks assembled by oncogenic EGFR and c-Met*. Proc Natl Acad Sci U S A, 2008. **105**(2): p. 692-7.

83. Bergstrom, J.D., B. Westermark, and N.E. Heldin, *Epidermal growth factor receptor signaling activates met in human anaplastic thyroid carcinoma cells*. Exp Cell Res, 2000. **259**(1): p. 293-9.

84. Ponzetto, C., et al., *c-met is amplified but not mutated in a cell line with an activated met tyrosine kinase*. Oncogene, 1991. **6**(4): p. 553-9.

85. Xu, L., et al., *Epidermal growth factor receptor regulates MET levels and invasiveness through hypoxia-inducible factor-1alpha in non-small cell lung cancer cells*. Oncogene, 2010.

86. Kong-Beltran, M., J. Stamos, and D. Wickramasinghe, *The Sema domain of Met is necessary for receptor dimerization and activation*. Cancer Cell, 2004. **6**(1): p. 75-84.

87. Mueller, K.L., et al., *Met and c-Src cooperate to compensate for loss of epidermal growth factor receptor kinase activity in breast cancer cells*. Cancer Res, 2008. **68**(9): p. 3314-22.

88. Siegfried, J.M., et al., *Signaling pathways involved in cyclooxygenase-2 induction by hepatocyte growth factor in non small-cell lung cancer*. Mol Pharmacol, 2007. **72**(3): p. 769-79.

89. Andermarcher, E., M.A. Surani, and E. Gherardi, *Co-expression of the HGF/SF and c-met genes during early mouse embryogenesis precedes reciprocal expression in adjacent tissues during organogenesis*. Dev Genet, 1996. **18**(3): p. 254-66.

90. Birchmeier, C. and E. Gherardi, *Developmental roles of HGF/SF and its receptor, the c-Met tyrosine kinase*. Trends Cell Biol, 1998. **8**(10): p. 404-10.

91. Schmidt, C., et al., *Scatter factor/hepatocyte growth factor is essential for liver development*. Nature, 1995. **373**(6516): p. 699-702.

92. Bladt, F., et al., *Essential role for the c-met receptor in the migration of myogenic precursor cells into the limb bud*. Nature, 1995. **376**(6543): p. 768-71.

93. Michalopoulos, G.K. and M.C. DeFrances, *Liver regeneration*. Science, 1997. **276**(5309): p. 60-6.

94. Nakamura, T., et al., *Myocardial protection from ischemia/reperfusion injury by endogenous and exogenous HGF*. J Clin Invest, 2000. **106**(12): p. 1511-9.

95. Sato, T., et al., *Focal enhancement of expression of c-Met/hepatocyte growth factor receptor in the myocardium in human myocardial infarction*. Cardiovasc Pathol, 2001. **10**(5): p. 235-40.

96. Rabkin, R., et al., *Hepatocyte growth factor receptor in acute tubular necrosis*. J Am Soc Nephrol, 2001. **12**(3): p. 531-40.

97. Park, M., et al., *Mechanism of met oncogene activation*. Cell, 1986. **45**(6): p. 895-904.

98. Comoglio, P.M., S. Giordano, and L. Trusolino, *Drug development of MET inhibitors: targeting oncogene addiction and expedience*. Nat Rev Drug Discov, 2008. **7**(6): p. 504-16.

99. Kong-Beltran, M., et al., *Somatic mutations lead to an oncogenic deletion of met in lung cancer*. Cancer Res, 2006. **66**(1): p. 283-9.

100. Ma, P.C., et al., *Functional expression and mutations of c-Met and its therapeutic inhibition with SU11274 and small interfering RNA in non-small cell lung cancer*. Cancer Res, 2005. **65**(4): p. 1479-88.

101. Stabile, L.P., et al., *Inhibition of human non-small cell lung tumors by a c-Met antisense/U6 expression plasmid strategy*. Gene Ther, 2004. **11**(3): p. 325-35.

102. Stabile, L.P., et al., *Therapeutic targeting of human hepatocyte growth factor with a single neutralizing monoclonal antibody reduces lung tumorigenesis*. Mol Cancer Ther, 2008. **7**(7): p. 1913-22.

103. Morotti, A., et al., *K252a inhibits the oncogenic properties of Met, the HGF receptor*. Oncogene, 2002. **21**(32): p. 4885-93.

104. Wang, X., et al., *Potent and selective inhibitors of the Met [hepatocyte growth factor/scatter factor (HGF/SF) receptor] tyrosine kinase block HGF/SF-induced tumor cell growth and invasion*. Mol Cancer Ther, 2003. **2**(11): p. 1085-92.

105. Christensen, J.G., et al., *A selective small molecule inhibitor of c-Met kinase inhibits c-Met-dependent phenotypes in vitro and exhibits cytoreductive antitumor activity in vivo*. Cancer Res, 2003. **63**(21): p. 7345-55.

106. Yamazaki, S., et al., *Pharmacokinetic-pharmacodynamic modeling of biomarker response and tumor growth inhibition to an orally available cMet kinase inhibitor in human tumor xenograft mouse models*. Drug Metab Dispos, 2008. **36**(7): p. 1267-74.

107. Zou, H.Y., et al., *An orally available small-molecule inhibitor of c-Met, PF-2341066, exhibits cytoreductive antitumor efficacy through antiproliferative and antiangiogenic mechanisms*. Cancer Res, 2007. **67**(9): p. 4408-17.

108. Kwak, E.L., et al., *Clinical activity observed in a phase 1 dose-escalation trial of an oral MET and ALK inhibitor, PF-02341066*. J Clin Oncol, 2009. **27**: p. Suppl.

109. Tang, Z., et al., *Dual MET-EGFR combinatorial inhibition against T790M-EGFR-mediated erlotinib-resistant lung cancer*. Br J Cancer, 2008. **99**(6): p. 911-22.

110. Yano, S., et al., *Hepatocyte growth factor induces gefitinib resistance of lung adenocarcinoma with epidermal growth factor receptor-activating mutations*. Cancer Res, 2008. **68**(22): p. 9479-87.

111. Fukui, T. and T. Mitsudomi, *Mutations in the epidermal growth factor receptor gene and effects of EGFR-tyrosine kinase inhibitors on lung cancers*. Gen Thorac Cardiovasc Surg, 2008. **56**(3): p. 97-103.

112. Soda, M., et al., *Identification of the transforming EML4-ALK fusion gene in non-small-cell lung cancer*. Nature, 2007. **448**(7153): p. 561-6.

113. Ladanyi, M. and W. Pao, *Lung adenocarcinoma: guiding EGFR-targeted therapy and beyond*. Mod Pathol, 2008. **21 Suppl 2**: p. S16-22.

114. Davies, H., et al., *Mutations of the BRAF gene in human cancer*. Nature, 2002. **417**(6892): p. 949-54.

115. Samuels, Y. and V.E. Velculescu, *Oncogenic mutations of PIK3CA in human cancers*. Cell Cycle, 2004. **3**(10): p. 1221-4.

116. Shannon, A.M., et al., *The mitogen-activated protein/extracellular signal-regulated kinase kinase 1/2 inhibitor AZD6244 (ARRY-142886) enhances the radiation responsiveness of lung and colorectal tumor xenografts*. Clin Cancer Res, 2009. **15**(21): p. 6619-29.

117. Siegfried, J.M., et al., *Evidence for autocrine actions of neuromedin B and gastrin-releasing peptide in non-small cell lung cancer*. Pulm Pharmacol Ther, 1999. **12**(5): p. 291-302.

118. Dempke, W.C., T. Suto, and M. Reck, *Targeted therapies for non-small cell lung cancer*. Lung Cancer. **67**(3): p. 257-74.

119. Klinghoffer, R.A., et al., *Src family kinases are required for integrin but not PDGFR signal transduction*. Embo J, 1999. **18**(9): p. 2459-71.

120. Goi, T., et al., *An EGF receptor/Ral-GTPase signaling cascade regulates c-Src activity and substrate specificity*. Embo J, 2000. **19**(4): p. 623-30.

121. Liu, X., et al., *Gastrin-releasing peptide activates Akt through the epidermal growth factor receptor pathway and abrogates the effect of gefitinib*. Exp Cell Res, 2007. **313**(7): p. 1361-72.

122. Pawson, T. and J.D. Scott, *Signaling through scaffold, anchoring, and adaptor proteins*. Science, 1997. **278**(5346): p. 2075-80.

123. Karni, R., et al., *Activated pp60c-Src leads to elevated hypoxia-inducible factor (HIF)-1alpha expression under normoxia*. J Biol Chem, 2002. **277**(45): p. 42919-25.

124. Weinstein, I.B. and A.K. Joe, *Mechanisms of disease: Oncogene addiction--a rationale for molecular targeting in cancer therapy*. Nat Clin Pract Oncol, 2006. **3**(8): p. 448-57.

125. Lu, Z., et al., *Downregulation of caveolin-1 function by EGF leads to the loss of E-cadherin, increased transcriptional activity of beta-catenin, and enhanced tumor cell invasion*. Cancer Cell, 2003. **4**(6): p. 499-515.

126. Lee, B.S., et al., *Hepatocyte growth factor induces delayed STAT3 phosphorylation through interleukin-6 expression*. Cell Signal, 2009. **21**(3): p. 419-27.

127. Ritter, C.A. and C.L. Arteaga, *The epidermal growth factor receptor-tyrosine kinase: a promising therapeutic target in solid tumors*. Semin Oncol, 2003. **30**(1 Suppl 1): p. 3-11.

128. Cai, T., et al., *Gab1 and SHP-2 promote Ras/MAPK regulation of epidermal growth and differentiation*. J Cell Biol, 2002. **159**(1): p. 103-12.

129. Silva, C.M., *Role of STATs as downstream signal transducers in Src family kinase-mediated tumorigenesis*. Oncogene, 2004. **23**(48): p. 8017-23.

130. Cao, X., et al., *Activation and association of Stat3 with Src in v-Src-transformed cell lines*. Mol Cell Biol, 1996. **16**(4): p. 1595-603.

131. Molina, J.R., A.A. Adjei, and J.R. Jett, *Advances in chemotherapy of non-small cell lung cancer*. Chest, 2006. **130**(4): p. 1211-9.

132. Nogawa, M., et al., *Monitoring luciferase-labeled cancer cell growth and metastasis in different in vivo models*. Cancer Lett, 2005. **217**(2): p. 243-53.

133. Puri, N. and R. Salgia, *Synergism of EGFR and c-Met pathways, cross-talk and inhibition, in non-small cell lung cancer*. J Carcinog, 2008. **7**: p. 9.

134. Lal, B., et al., *EGFRvIII and c-Met pathway inhibitors synergize against PTEN-null/EGFRvIII+ glioblastoma xenografts*. Mol Cancer Ther, 2009. **8**(7): p. 1751-60.

135. Kawaguchi, K., et al., *Combined inhibition of MET and EGFR suppresses proliferation of malignant mesothelioma cells*. Carcinogenesis, 2009. **30**(7): p. 1097-105.

136. I. Laux, J.G., R. Just, K. Brady, J. Li, B. Schwartz, R. Savage, E. Garmey, L. Rosen, *Phase I dose escalation trial (ARQ 197-111) evaluating combination of selective c-Met inhibitor ARQ 197 and erlotinib*.. J Clin Oncol, 2009. **27**(15s): p. Abstract 3549

137. Schiller JH, A.W., Brugger D, et al., *Results from ARQ 197-209: A global randomized placebo-controlled phase II clinical trial of erlotinib plus ARQ 197 versus erlotinib plus placebo in previously treated EGFR inhibitor-naive patients with locally advanced or metastatic non-small cell lung cancer (NSCLC)*. J Clin Oncol, 2010. **282**(18s: Abstract LBA750).

138. Stommel, J.M., et al., *Coactivation of receptor tyrosine kinases affects the response of tumor cells to targeted therapies*. Science, 2007. **318**(5848): p. 287-90.

139. Wang, D., et al., *Clinical experience of MEK inhibitors in cancer therapy*. Biochim Biophys Acta, 2007. **1773**(8): p. 1248-55.

140. Maira, S.M., et al., *PI3K inhibitors for cancer treatment: where do we stand?* Biochem Soc Trans, 2009. **37**(Pt 1): p. 265-72.

141. Jun, H.T., et al., *AMG 102, a fully human anti-hepatocyte growth factor/scatter factor neutralizing antibody, enhances the efficacy of temozolomide or docetaxel in U-87 MG cells and xenografts*. Clin Cancer Res, 2007. **13**(22 Pt 1): p. 6735-42.

142. Kim, L.C., L. Song, and E.B. Haura, *Src kinases as therapeutic targets for cancer*. Nat Rev Clin Oncol, 2009. **6**(10): p. 587-95.

143. Li, J., et al., *A chemical and phosphoproteomic characterization of dasatinib action in lung cancer*. Nat Chem Biol. **6**(4): p. 291-9.

144. Kolch, W., *Coordinating ERK/MAPK signalling through scaffolds and inhibitors*. Nat Rev Mol Cell Biol, 2005. **6**(11): p. 827-37.

145. Villa-Moruzzi, E., et al., *Protein tyrosine phosphatase PTP-S binds to the juxtamembrane region of the hepatocyte growth factor receptor Met*. Biochem J, 1998. **336 (Pt 1)**: p. 235-9.

146. Sheth, P.R. and S.J. Watowich, *Oligomerization-induced differential dephosphorylation of c-Met receptor tyrosine kinase*. Biochemistry, 2005. **44**(33): p. 10984-93.